

Photon Spheres and Sonic Horizons in Black Holes from Supergravity and Other Theories

M. Cvetič^{1,2,6}, G.W. Gibbons^{2,3,5} and C.N. Pope^{1,3,4,5}

¹ *Department of Physics, Beijing Normal University, Beijing, 100875, China*

² *Department of Physics and Astronomy,*

University of Pennsylvania, Philadelphia, PA 19104, USA

³ *DAMTP, Centre for Mathematical Sciences,*

Cambridge University, Wilberforce Road, Cambridge CB3 0WA, UK

⁴ *Mitchell Institute for Fundamental Physics and Astronomy,*

Texas A&M University, College Station, TX 77843-4242, USA

⁵ *Laboratoire de Mathématiques et Physique Théorique, CNRS-UMR 7350, Université de Tours,*

Parc de Grandmont, 37200 Tours, France

⁶ *Center for Applied Mathematics and Theoretical Physics,*

University of Maribor, SI2000 Maribor, Slovenia

ABSTRACT

We study closed photon orbits in spherically-symmetric static solutions of supergravity theories, a Horndeski theory, and a theory of quintessence. These orbits lie in what we shall call a *photon sphere* (*anti-photon sphere*) if the orbit is unstable (stable). We show that in all the asymptotically flat solutions we examine that admit a regular event horizon, and whose energy-momentum tensor satisfies the strong energy condition, there is one and only one photon sphere outside the event horizon. We give an example of a Horndeski theory black hole (whose energy-momentum tensor violates the strong energy condition) whose metric admits both a photon sphere and an anti-photon sphere. The uniqueness and non-existence also holds for asymptotically anti-de Sitter solutions in gauged supergravity. The latter also exhibit the projective symmetry that was first discovered for the Schwarzschild-de Sitter metrics: the unparameterised null geodesics are the same as when the cosmological or gauge coupling constant vanishes. We also study the closely related problem of accretion flows by perfect fluids in these metrics. For a radiation fluid, Bondi's sonic horizon coincides with the photon sphere. For a general polytropic equation of state this is not the case. Finally we exhibit counterexamples to a conjecture of Hod's.

Contents

1	Introduction	3
2	General Theory	6
2.1	Notation and basic formulae	6
2.2	Gauss curvature	7
2.3	Hod's theorem and a conjecture	11
2.4	Geodesics and projective symmetry	14
2.5	York-Hawking-Page phase transition	16
3	Static Spherically Symmetric STU Black Holes in Four Dimensions	17
3.1	Static four-charge STU black holes	17
3.2	Photon spheres	19
3.3	Projective symmetry for the general STU black holes	21
3.4	Dyonic solutions of the gauged STU model	23
4	Einstein-Maxwell-Dilaton Black Holes	24
4.1	Static black holes in EMD theories	24
4.2	Photon spheres and Hod's conjecture	26
4.3	Projective symmetry for the dilatonic black holes	28
5	Black Holes in Horndeski Gravity	29
6	Quintessence Black Holes	31
7	Higher Dimensions	33
7.1	Five dimensions	33
7.2	Seven dimensions	34
8	Conclusions	35
9	Acknowledgements	36
A	k-Essence and Irrotational Relativistic Fluids	36
A.1	Thermodynamics	37
A.2	Entropy current as Noether current	38
A.3	Black hole accretion and emission	39

1 Introduction

By Fermat’s principle, the study of null geodesics in a static $(d + 1)$ -dimensional spacetime with metric

$$ds_{d+1}^2 = -e^{2U(x)} dt^2 + g_{ij} dx^i dx^j \quad (1.1)$$

may be reduced to the study of the geodesics of the spatial manifold equipped with the conformally rescaled “optical metric”

$$ds_{\text{opt}}^2 = \gamma_{ij} dx^i dx^j = e^{-2U} g_{ij} dx^i dx^j . \quad (1.2)$$

The optical metric encodes more physical information than just the optical properties of the spacetime. As we shall show later, it is relevant to stability questions and to the existence of York-Hawking-Page type phase transitions. Much more is known and is accessible in the spherically symmetric case than for a general metric, and that is the situation we shall consider in this paper. A great many spherically symmetric static solutions of Einstein’s equations are known, including those describing black holes. In particular, in recent years there has been a great deal of activity constructing exact solutions of the supergravity and related equations of motion for spatial dimensions $d = 3$ and higher. Since their stress-energy tensors, at least without cosmological terms, satisfy the weak, dominant and strong energy conditions, one is assured that the properties of such solutions are not artefacts of the matter content’s being un-physical.

The motivations for our study include:

- In the spherically symmetric case it is well known that unstable circular null geodesics are possible, and that these circular null geodesics lie on a “photon sphere.” In principle “anti-photon spheres,” are also possible¹. In such cases, the circular null geodesics are stable. These are much less familiar, and to our knowledge there are no known asymptotically-flat examples that are regular outside a regular event horizon and with matter content satisfying all of the three energy conditions mentioned above. Examples are known, however, in cases where naked singularities are present [1]. It has been suggested that the existence of an anti-photon sphere is an indication that the solution may be unstable. [2, 3].
- A less obvious aspect of photon spheres and anti-photon spheres is that they signal the possibility of a York-Hawking-Page phase transition [4–6]. This occurs because the

¹At an early stage of the work reported here we were accustomed to refer to a sphere of stable geodesics as a “whispering gallery.” However the analogy with more mundane whispering galleries is not that close. As pointed out to us by Claude Warnick, the term “whispering gallery” is more appropriately applied to the conformal boundary of anti-de Sitter spacetime.

Dirichlet boundary-value problem in Euclidean quantum gravity may have multiple solutions that jump in number when the boundary passes through a photon sphere or an anti-photon sphere [7].

- A number of conjectures have been made about photon spheres, and it is of interest to check them against our examples. In particular, we found that a conjecture of Hod [8] concerning a lower bound on the optical radius of a photon sphere, is violated for dilatonic black holes with the dilaton coupling $a^2 > 1$ and for STU black holes with fewer than two charges turned on. On the other hand, a theorem of Hod [9], concerning an upper bound on area-coordinate radius of a photon sphere, is confirmed both for the STU black holes and dilatonic black holes.
- It has been known for some time that the existence of photon spheres affects the optical appearance of collapsing stars [10], and gives rise to shadows [11]. It is also known that the optical radius governs the high-frequency behaviour of the photon absorption cross section, and the high frequency spectrum of quasi-normal modes [12, 13].
- While the optical metric governs the behaviour of null geodesics parameterised by optical length, it may happen that two different metrics admit the same unparameterised null geodesics. This “projective equivalence” actually occurs for the Schwarzschild-de Sitter or Kottler metric. The unparameterised null geodesics are independent of the cosmological constant [14–16]. Surprisingly, we find that this phenomenon is a rather general feature of the solutions we study.
- In the spherically symmetric case, each geodesic lies in a reflection-symmetric equatorial surface. The behaviour of the geodesics is heavily influenced by the sign of the Gauss curvature of this surface [17–19], and in the asymptotically-flat case this allows a rapid evaluation of the light deflection at large impact parameter [17, 18]. The Gauss curvature also determines the shape, and indeed the very possibility, of isometrically embedding the surface into Euclidean space as a surface of revolution so as to provide an analogue model of black holes [20, 21]. There is a close connection between the sign of the Gauss curvature and the existence of photon and anti-photon spheres.
- In the spherically-symmetric case the steady radial accretion or emission of a test perfect fluid must make a transition from sub-sonic to super-sonic flow through a so-called Bondi surface [20]. For a radiation fluid for which the pressure is one third of the energy density, the Bondi surface and photon surface coincide. As we shall show in an appendix, for an equation of state of the form $P = w\rho$ where w is a constant, the Bondi radius is located at a stationary point of $\frac{(-g_{tt}(R))^{p-1}}{R^2}$, where $w = \frac{1}{2p-1}$. If

$p = 2$ then $w = 3$ and this gives the same condition for the existence of a photon sphere.

The plan of the paper is as follows.

In §2 we review in outline the general theory of the optical metric of a static spherically symmetric spacetime and its applications. Much, but not all, of this can be found scattered in the existing literature but we thought it helpful to assemble in one place and we have used this opportunity to establish our notation. In particular appears to be no consensus one what to call what we shall refer to as photon sphere and anti-photon sphere and so we have spelled out in detail the usage adopted here.

In §3 we discuss in detail the static spherically symmetric solutions of four-dimensional gauged and ungauged STU supergravity theory. After giving the metrics in a standard radial coordinate r we introduce, in the ungauged case, an isotropic coordinate ρ which allows us to assign them an effective refractive index $n(\rho)$. In the non-extremal case, when there is an event horizon, we are able to locate their unique photon sphere and establish that that its location in the coordinate r does not depend upon the gauge coupling constant. We also verify that for non-extremal black holes the a theorem of Hod's [9] is satisfied, while Hod's conjecture [8] is violated if fewer than two charges are turned on. In the ultra-extremal case, which has naked singularities, we found that for a range of charges there is both a photon sphere and an anti-photon sphere. We then investigate, by introducing an appropriate Binet type coordinate u , analogous to that used in the central orbit problems of elementary non-relativistic dynamics, that the projective properties of the optical metric, i.e. its unparameterised geodesics, do not depend on the gauge coupling constant g . This result is confirmed at a more covariant level by calculating the Weyl projective tensor and finding it to be independent of g . We conclude §3 by showing that similar results hold for a class of dyonic solutions of gauged supergravity theories.

In §4 we extend these results to static spherically symmetric solutions of Einstein-Maxwell-Dilaton theory in four spacetime dimensions, which depend upon an arbitrary Maxwell-dilaton coupling constant a . These theories may be thought of as having a spacetime-dependent electric permittivity $\epsilon = \exp(-2a\phi)$, where ϕ is the dilaton field, while preserving local Lorentz invariance. These solutions permit a check that the conjecture of Hod in [8] is violated for $a^2 > 1$, while Hod's theorem [9] is obeyed.

In §5 we consider the static spherically symmetric solutions of a particularly simple Horndeski theory in which a metric $g_{\mu\nu}$ is coupled to a scalar χ . For certain values of the constants entering the solution we find that the optical geometry of the metric $g_{\mu\nu}$ admits both a photon sphere and an anti-photon sphere outside its Killing horizon.

In §6 we treat a class of quintessence black holes due to Kiselev. They admit both a black

hole horizon and an analogue of the cosmological horizon that occurs in de Sitter spacetime. We find that, just as in the case of de Sitter black holes, there is just a single photon sphere between the two horizons.

In §7 we provide a brief discussion of some static hyper-spherically symmetric solutions of gauged supergravity theories in five and seven spacetime dimensions. As in four spacetime dimensions we find at most a single photon hyper-sphere whose location is independent of the gauged coupling constant g .

Finally in an appendix we outline a formalism for irrotational perfect fluids using a velocity potential ψ , which may be regarded as k -essence. Using this we are able to give a novel treatment of accretion onto black holes, and to use it to locate the sonic or Bondi radius, which is the acoustic analogue of a photon surface.

2 General Theory

2.1 Notation and basic formulae

In what follows we shall find it convenient to express the optical metric in terms of various different radial variables. We shall use r for a generic radial variable, but reserve r_\star for the radial optical distance or Regge-Wheeler tortoise coordinate, and R_{opt} , with $C_{\text{opt}} = 2\pi R_{\text{opt}}$, such that the optical metric (1.2) becomes

$$ds_{\text{opt}}^2 = dr_\star^2 + R_{\text{opt}}^2 d\Omega_{d-1}^2, \quad (2.1)$$

where $d\Omega_{d-1}^2$ is the unit metric on \mathbb{S}^{d-1} . Therefore

$$R_{\text{opt}} = e^{-U} R, \quad (2.2)$$

where R is the “area distance,” such that the area of a 2-sphere measured in the physical spacetime metric is $4\pi R^2$. Restricting (2.1) to an equatorial 2-surface gives

$$ds_{\text{opt}}^2| = dr_\star^2 + R_{\text{opt}}^2 d\phi^2, \quad 0 \leq \phi < 2\pi. \quad (2.3)$$

The Gauss curvature is

$$K_{\text{opt}} = -\frac{1}{R_{\text{opt}}} \frac{d^2 R_{\text{opt}}}{dr_\star^2}. \quad (2.4)$$

Any spherically symmetric metric is conformally flat, and so one may also introduce an isotropic coordinate ρ such that

$$ds_{\text{opt}}^2 = n^2(\rho) \left(d\rho^2 + \rho^2 d\Omega_{d-1}^2 \right). \quad (2.5)$$

The quantity n may be interpreted in the language of elementary optics in Euclidean space as the refractive index or slowness, so that the “speed of light” $v = \frac{d\rho}{dt}$ in the coordinates (t, ρ) is given by $v = \frac{1}{n}$. Thus we have

$$R_{\text{opt}} = n\rho = \frac{\rho}{v}. \quad (2.6)$$

If $dw = -\frac{dr_\star}{R_{\text{opt}}^2} = -\frac{d\rho}{n\rho^2}$, then, as we shall see in detail later, unparameterised geodesics of the optical metric satisfy an equation similar to Binet’s equation for central orbits,

$$\frac{d^2w}{d\phi^2} = -\frac{1}{2} \frac{d}{dw} \frac{1}{R_{\text{opt}}^2}. \quad (2.7)$$

Circular geodesics therefore correspond to extremals of the optical circumference at points $r = \bar{r}$, i.e. for which

$$R'_{\text{opt}}|_{r=\bar{r}} = 0. \quad (2.8)$$

We have an unstable photon sphere if $R''_{\text{opt}}|_{r=\bar{r}} > 0$, and a stable photon sphere, where light propagation is analogous to the acoustic propagation in a SOFAR channel, if $R''_{\text{opt}}|_{r=\bar{r}} < 0$.²

In the case of an asymptotically-flat black hole, R_{opt} goes to infinity both at infinity and also at a regular horizon, and so there is always at least one photon sphere. In general one might expect that there should be one more minimum than there are maxima, that the outer and inner extrema should be minima, and that the inner extrema to have k maxima alternating with $k - 1$ minima, there being $2k + 1$ extrema in all. From (2.6) it follows that (2.8) is equivalent to

$$\frac{dv}{d\rho} = \frac{v}{\rho}. \quad (2.9)$$

Thus if we plot the speed $v = \frac{1}{n}$ against ρ then photon and anti-photon spheres correspond to points on the graph at which a straight line through the origin is tangent to it. If the straight line touches the graph from above we have a photon sphere. If it touches it from below, an anti-photon-sphere. The slope at those points $\rho = \bar{\rho}$ then equals the inverse optical radius, $R_{\text{opt}}(\bar{\rho})^{-1}$.

2.2 Gauss curvature

In the usual case that there is just one photon sphere and the metric is asymptotically flat, we expect the graph of $R_{\text{opt}}(r_\star)$ to be convex, in which case from (2.4) we see that the Gauss curvature K_{opt} is negative. This allows a qualitative analysis of the geodesics using the Gauss-Bonnet theorem [17, 18]. It also has implications for boundary rigidity and

²A SOFAR (Sound Fixing and Ranging) channel arises in a horizontal layer in the ocean where the speed of sound attains a local maximum. This acts like an acoustic waveguide, in which low-frequency sound waves can travel large distances with little attenuation [23–25].

the related inverse problem, which in turn connects with holography and the AdS/CFT correspondence, as was observed in [26]. Our situation relates to what geometers call *lens rigidity*, a subject which also arises in connection with invisibility cloaks, and related devices. The strongest general mathematical result in this area is directly applicable to the our present work.

2.2.1 Lens Rigidity and Holography

The basic idea is to idealise a static optical lensing device as a compact connected n -dimensional Riemannian manifold $\{M, g\}$ with a, not necessarily connected, boundary ∂M , with light rays described as geodesics in the optical metric g . If ν is the *inward* pointing normal, we define the $(2d - 2)$ -dimensional space $U^+\partial M$ as the set of positions $x \in \partial M$ and inward pointing unit vectors v such that $g(\nu, v) \geq 0$, and $U^-\partial M$ as the set of positions $x \in \partial M$ and outward pointing unit vectors v such that $g(\nu, v) \neq 0$. Then for all geodesics with initial tangent vector $v \in U^+\partial M$ which after a finite time $\tau > 0$ first arrive at ∂M , we get a map $S : U^+\partial M \rightarrow U^-\partial M$ called the *scattering map* or *scattering data*. Note that the scattering map is not defined if $\tau = \infty$, in which case we say that the geodesic is *trapped* and may be defined as the identity if $\tau = 0$. The scattering map S and the time function $\tau : U^+\partial M \rightarrow \mathbb{R}_+$ are referred to as the *lens data*. There is an obvious notion of equivalence, under diffeomorphism of the boundary, of the notions of scattering map and lens data. The optical device is said to be *scattering rigid* or *lens rigid* if the scattering data or lens data determine the Riemannian manifold $\{M, g\}$ up diffeomorphism. The freedom to make such diffeomorphisms is the essential principle behind the construction of optical cloaking devices. Lens rigidity, if it holds, is the statement that that is the *only* freedom.

Various theorems have been proved that demonstrate lens rigidity under the restrictive assumption that the Riemannian manifold $\{M, g\}$ is *simple*; that is, the boundary ∂M is strictly convex and for all $x \in M$ the exponential map $\exp_x : \exp_x^{-1}(M) \rightarrow M$ is a diffeomorphism. However if trapping takes place, then the simplicity assumption does not hold. There are comparatively few results in that case. Since trapping typically takes place for light rays around black holes, this is an important gap if one wishes to apply these results to the optical metrics of static spacetimes. However, recently an important advance has been made by Croke [27] (see also [28]), who shows that lens rigidity holds if

- $d = 2$,
- topologically $M \equiv S^1 \times I$, where I is the unit interval,
- the boundary ∂M is convex,
- the Gauss curvature K of M is negative.

2.2.2 Isometric Embedding

Near a horizon one has [19] $K_{\text{opt}} = \kappa$, where κ is the surface gravity of the horizon, which is of course a constant over the horizon. This has consequences for the popular way of visualizing the geometry of a two-dimensional Riemannian manifold. This is to isometrically embed the metric into Euclidean space. If the metric is invariant under a circle action, one may attempt to embed it as a surface of revolution. If the embedding is

$$(r_*, \phi) \rightarrow (x, y, z) = (R_{\text{opt}}(r_*) \cos \phi, R_{\text{opt}}(r_*) \sin \phi, z(r_*)), \quad (2.10)$$

then $z(r_*)$ satisfies the ordinary differential equation:

$$\left(\frac{dz}{dr_*}\right)^2 = 1 - \left(\frac{R_{\text{opt}}}{dr_*}\right)^2. \quad (2.11)$$

A solution will exist as long as

$$\left(\frac{R_{\text{opt}}}{dr_*}\right)^2 \leq 1. \quad (2.12)$$

For the Schwarzschild solution, this will be true as long as [20]

$$R \geq \frac{9}{8}M. \quad (2.13)$$

In [21], the obstruction (2.12) was shown to apply to analogue models of black holes constructed from graphene sheets. In terms of the isotropic coordinate ρ and the ray velocity v , (2.12) becomes

$$\left(1 - \frac{\rho}{v} \frac{dv}{d\rho}\right)^2 \leq 1. \quad (2.14)$$

2.2.3 Energy conditions and monotonicity of redshift

The *weak energy condition* implies

$$T_{\hat{t}\hat{t}} \geq 0. \quad (2.15)$$

If the weak energy condition holds, then the Misner-Sharp mass $M(R)$ is non-decreasing and bounded above by the ADM mass $M_{ADM} = M(\infty)$:

$$M(R) \leq M_{ADM}. \quad (2.16)$$

The *dominant energy condition* implies that

$$T_{\hat{t}\hat{t}} - |T_{\hat{R}\hat{R}}| \geq 0, \quad (2.17)$$

which implies the weak energy condition, as well as

$$T_{\hat{t}\hat{t}} + T_{\hat{R}\hat{R}} \geq 0. \quad (2.18)$$

The *Strong energy condition* implies

$$T_{\hat{t}\hat{t}} + T_{\hat{R}\hat{R}} + T_{\hat{\theta}\hat{\theta}} + T_{\hat{\phi}\hat{\phi}} \geq 0. \quad (2.19)$$

The *Positive radial pressure condition* implies

$$T_{\hat{R}\hat{R}} \geq 0. \quad (2.20)$$

The *Positive or Negative trace conditions* are

$$T \geq 0, \quad \text{or} \quad T \leq 0, \quad \text{respectively.} \quad (2.21)$$

Any static solution of the Einstein equations coupled to scalars and vectors, and with non-positive potentials for the scalars and a negative cosmological term, satisfies the negative trace condition.

The $R_{\hat{t}\hat{t}}$ orthonormal Ricci-tensor component of the d -dimensional static metric

$$ds^2 = -\Phi^2 dt^2 + g_{ij} dx^i dx^j, \quad (2.22)$$

where Φ and g_{ij} are independent of t , is given by

$$R_{\hat{t}\hat{t}} = \Phi^{-1} \nabla_g^2 \Phi, \quad (2.23)$$

where ∇_g^2 is the Laplace-Beltrami operator for the spatial metric g_{ij} . From this, it follows that the Einstein equations $R_{\mu\nu} - \frac{1}{2}Rg_{\mu\nu} = 8\pi T_{\mu\nu}$ imply (generalising the $d = 4$ result of ref. [29])

$$\nabla_g^2 \Phi = \frac{8\pi\Phi}{d-2} \left[\frac{d-4}{d-2} T_{\hat{t}\hat{t}} + (T_{\hat{t}\hat{t}} + \sum_i T_{\hat{i}\hat{i}}) \right]. \quad (2.24)$$

(As a check on signs, note that in the Newtonian limit, where we ignore $T_{\hat{i}\hat{i}}$, then $\Phi = e^U \approx 1 + U + \dots$ where U is the Newtonian potential and we recover the Poisson equation.)

In the case of a four-dimensional metric with spherical symmetry this gives

$$\frac{1}{\sqrt{g}} \frac{d}{dr} \left(\sqrt{g} g^{rr} \frac{d\Phi}{dr} \right) = 4\pi\Phi (T_{\hat{t}\hat{t}} + T_{\hat{r}\hat{r}} + T_{\hat{\theta}\hat{\theta}} + T_{\hat{\phi}\hat{\phi}}), \quad (2.25)$$

where $g = \det g_{ij}$. Thus

$$\sqrt{g} g^{rr} \frac{d\Phi}{dr} = \frac{\kappa A_H}{4\pi} + \int_{r_H}^r 4\pi\Phi (T_{\hat{t}\hat{t}} + T_{\hat{r}\hat{r}} + T_{\hat{\theta}\hat{\theta}} + T_{\hat{\phi}\hat{\phi}}) \sqrt{g} dr, \quad (2.26)$$

where A_H is the area and κ the surface gravity of the horizon. By the strong energy condition, the integral on the right-hand side is non-negative, and hence $|g_{tt}|$ is monotonically increasing. Note that if there is a negative cosmological constant, the same conclusion, *a fortiori*, follows. If we take the limit of (2.26) as $r \rightarrow \infty$ we obtain a form of the Smarr formula.

2.3 Hod's theorem and a conjecture

In this subsection, we shall mainly use the area coordinate R as the radial variable. As in the earlier discussion, we shall denote with a bar the value of the radial coordinate that corresponds to a stationary point of the optical radius; i.e. a photon sphere or anti-photon sphere.

We consider the static metric

$$\begin{aligned} ds^2 &= -e^{2\gamma(R)} \left(1 - \frac{2M(R)}{R}\right) dt^2 + \frac{dR^2}{\left(1 - \frac{2M(R)}{R}\right)} + R^2(d\theta^2 + \sin^2\theta d\phi^2), \\ &= -e^{2U} dt^2 + \frac{dR^2}{\left(1 - \frac{2M(R)}{R}\right)} + R^2(d\theta^2 + \sin^2\theta d\phi^2), \end{aligned} \quad (2.27)$$

where $M(R)$ is the Misner-Sharp mass. It satisfies

$$\frac{dM}{dR} = 4\pi R^2 T_{\hat{t}\hat{t}}, \quad (2.28)$$

$$\frac{d\gamma}{dR} = 4\pi R \frac{(T_{\hat{t}\hat{t}} + T_{\hat{R}\hat{R}})}{\left(1 - \frac{2M(R)}{R}\right)}, \quad (2.29)$$

$$\frac{d(R^4 T_{\hat{R}\hat{R}})}{dR} = -\frac{F}{\left(1 - 2\frac{M(R)}{R}\right)} (T_{\hat{t}\hat{t}} + T_{\hat{R}\hat{R}}) + RT, \quad (2.30)$$

where

$$T = T_{\mu}^{\mu} = -T_{\hat{t}\hat{t}} + T_{\hat{R}\hat{R}} + T_{\hat{\theta}\hat{\theta}} + T_{\hat{\phi}\hat{\phi}} \quad (2.31)$$

and

$$F = 3M(R) - R + 4\pi R^2 T_{\hat{R}\hat{R}}. \quad (2.32)$$

In the case of an isotropic fluid we have

$$T_{\hat{t}\hat{t}} = \rho, \quad T_{\hat{R}\hat{R}} = T_{\hat{\theta}\hat{\theta}} = T_{\hat{\phi}\hat{\phi}} = P, \quad (2.33)$$

where ρ is the energy density and P is the pressure. Our equations then reduce to the Tolman-Oppenheimer-Volkov equations

$$\frac{dP}{dR} = -(\rho + P) \frac{M(R) + 4\pi R^3 P}{R^2 \left(1 - \frac{2M(R)}{R}\right)} \quad (2.34)$$

$$\frac{dU}{dR} = \frac{M(R) + 4\pi R^3 P}{R^2 \left(1 - \frac{2M(R)}{R}\right)} \quad (2.35)$$

whence

$$dU = -\frac{dP}{\rho + P}. \quad (2.36)$$

2.3.1 Hod's photon sphere theorems

In the coordinates we are using, the optical radius for the metric (2.27) is given by

$$R_{\text{opt}}(R) = Re^{-U} = Re^{-\gamma} \left(1 - \frac{2M(R)}{R}\right)^{-\frac{1}{2}}. \quad (2.37)$$

It follows from (2.28) and (2.29) that

$$\frac{d(R_{\text{opt}}^{-2})}{dR} = \frac{2}{R^4} e^{2\gamma} F, \quad (2.38)$$

where F is defined in eqn (2.32). At either a photon sphere or an anti-photon sphere, we have $\frac{dR_{\text{opt}}}{dR} = 0$ and hence

$$F = 0, \quad \Rightarrow \quad \bar{R} = 3M(\bar{R}) + 4\pi\bar{R}^3 T_{\hat{R}\hat{R}}(\bar{R}). \quad (2.39)$$

It is perhaps worth remarking that for an isotropic medium for which the Tolman-Oppenheimer-Volkov equations hold, eqn (2.39) follows directly from (2.35), by noting from $R_{\text{opt}} = Re^{-U}$ that $dR_{\text{opt}}/dR = 0$ implies

$$\frac{1}{\bar{R}} = \frac{dU}{dR} \Big|_{R=\bar{R}}. \quad (2.40)$$

Returning to the general non-isotropic case, and considering a black hole, then at the horizon $R = R_H$ the component $T_{\hat{R}\hat{R}}$ of the energy-momentum tensor vanishes,

$$T_{\hat{R}\hat{R}}(R_H) = 0, \quad (2.41)$$

and R_{opt} blows up:

$$\lim_{R \downarrow R_H} R_{\text{opt}}(R) = \infty. \quad (2.42)$$

Thus F is negative near the horizon [9]. On the other hand F is positive near infinity. Thus there must be at least one value of $R = \bar{R}$ for which $F(\bar{R}) = 0$. Moreover the smallest such value, \bar{R}_{min} , must be a local minimum, which corresponds to an unstable photon sphere rather than a stable anti-photon sphere. Thus F is negative for $R_H < R < \bar{R}_{\text{min}}$. Now if we assume the negative trace condition, it follows from (2.30) that

$$T_{\hat{R}\hat{R}}(\bar{R}_{\text{min}}) < 0, \quad (2.43)$$

and hence from (2.39), we have

$$R_H < \bar{R}_{\text{min}} \leq 3M(\bar{R}_{\text{min}}) \leq 3M_{ADM}. \quad (2.44)$$

In particular, this implies Hod's theorem [9], namely, that provided the trace of the energy-momentum tensor is negative, and that the dominant energy condition holds, then

$$\bar{R}_{\text{min}} \leq 3M_{ADM}. \quad (2.45)$$

A generalisation of (2.45) to higher dimensions has been given in [22].

A further inequality proved by Hod in [9] is as follows. Assuming the dominant energy condition, it follows from (2.29) that $d\gamma/dR \geq 0$, and hence, since $\gamma = 0$ at infinity, $\gamma \leq 0$. Thus, from (2.37), we have

$$R_{\text{opt}} \geq R \left(1 - \frac{2M(R)}{R}\right)^{-1/2}. \quad (2.46)$$

From (2.44) we have $\bar{R}_{\text{min}} \leq 3M(\bar{R}_{\text{min}})$, and hence

$$R_{\text{opt}}(\bar{R}) \geq \sqrt{3}\bar{R}. \quad (2.47)$$

The question of whether the closed photon orbit is stable or unstable is governed by the sign of the second derivative of R_{opt} at the radius of the orbit. Using (2.28), (2.29) and (2.30), it follows, after imposing the condition (2.39) that determines the orbital radius, that on the orbit we shall have

$$\frac{d^2 R_{\text{opt}}^{-2}}{dR^2} = \frac{2e^{2\gamma}}{R^4} F', \quad (2.48)$$

with

$$F' \equiv \frac{dF}{dR} = -1 + 4\pi R^2 (2T_{\hat{t}\hat{t}} + T_{\hat{\theta}\hat{\theta}} + T_{\hat{\phi}\hat{\phi}}), \quad (2.49)$$

which is to be evaluated at the photon radius $R = \bar{R}$. The orbit is unstable (a photon sphere) if F' is negative, and stable (an anti-photon sphere) if F' is positive.

As we show in later sections, in the case of theories such as supergravities, where the energy-momentum tensors satisfy all the relevant energy conditions, we find that there is always exactly one closed photon orbit outside the horizon of a regular black hole, and it is always unstable, corresponding to a photon sphere. However, it does not appear to be obvious on general grounds from (2.49) that the energy conditions are in themselves sufficient to guarantee the negativity of F' at the photon orbit. We show also that in the case of ultra-extremal black holes (where there is a naked singularity), there can be more than one photon orbit, with stable as well as unstable orbits. We also study other examples with more exotic matter that does not obey all the usual energy conditions, and we show that in such cases there can exist multiple photon orbits outside an horizon.

2.3.2 Hod's conjecture

Hod [8, 30] has made some conjectures about photon surfaces in spherically-symmetric geometries, and circular null geodesics in stationary spacetimes. A special case of a conjecture in [8] is that the optical radius R_{opt} of a photon surface in an asymptotically flat spacetime with ADM mass M_{ADM} satisfies

$$R_{\text{opt}} \geq 2M_{ADM}. \quad (2.50)$$

Both of Hod's theorems (2.45) and (2.47), and the conjecture (2.50) may be tested by the methods of this paper. Unsurprisingly, the theorems hold in all the examples satisfying the assumptions under which they were derived. We find that the conjecture (2.50) is in fact violated in some circumstances. As we shall discuss later, we find that in the four-charge black holes of four-dimensional STU supergravity, the conjecture holds for the case where all the charges are equal (Reissner-Nordström), and for pairwise equal charges (string theory case, $a^2 = 1$). However, the conjectured inequality (2.50) is not obeyed in the case where only one charge is non-vanishing (Kaluza-Klein, $a = 3$). In section 4 we show that it is violated also in Einstein-Maxwell-Dilaton theories with $a^2 > 1$.

2.4 Geodesics and projective symmetry

The geodesics of the optical metric have two constants of the motion:

$$\text{Angular momentum} \quad R_{\text{opt}}^2 \frac{d\phi}{ds_{\text{opt}}} = h. \quad (2.51)$$

$$\text{Energy} \quad \left(\frac{dr_{\star}}{ds_{\text{opt}}}\right)^2 + R_{\text{opt}}^2 \left(\frac{d\phi}{ds_{\text{opt}}}\right)^2 = 1, \quad (2.52)$$

whence

$$\left(\frac{dr_{\star}}{R_{\text{opt}}^2 d\phi}\right)^2 + \frac{1}{R_{\text{opt}}^2} = \frac{1}{h^2} = \left(\frac{dw}{d\phi}\right)^2 + \frac{1}{R_{\text{opt}}^2}. \quad (2.53)$$

If one differentiates (2.53) with respect to w one obtains the Binet type equation (2.7).

An alternative procedure is to adopt isotropic coordinates, in which case the geodesic equations may be cast into the standard form for a central orbit problem. Thus we make the standard redefinition $u = \frac{1}{\rho}$, and find that (2.53) becomes

$$\left(\frac{du}{d\phi}\right)^2 + u^2 = \frac{n^2}{h^2}, \quad (2.54)$$

so that

$$\frac{d^2u}{d\phi^2} + u = \frac{P}{h^2 u^2} \quad (2.55)$$

with

$$P = -\frac{1}{2} \frac{\partial n^2}{\partial \rho}, \quad (2.56)$$

and where P is the acceleration of the particle towards the origin. Equation (2.55) is the standard form of Binet's equation for central orbits.

2.4.1 Projective symmetry

Differentiating (2.53) with respect to u yields (2.7), from which it follows that two metrics for which $\frac{1}{R_{\text{opt}}^2}$ differ by a constant have the same unparameterised geodesics and are thus

projectively equivalent, as explained in [15] where it was shown that the Weyl projective tensors of two such optical metrics are the same.

A projective symmetry of this type was first noticed for the Kottler metric, but not in this language in [14]. We shall see later that, rather remarkably, all the gauged supergravity models that we study admit a projective symmetry of this type.

2.4.2 Shadows

For any curve, the angle δ made with the radial direction satisfies

$$\cot \delta = \frac{1}{R_{\text{opt}}} \frac{dr_{\star}}{d\phi}. \quad (2.57)$$

For a geodesic it follows from (2.53) that

$$\sin \delta = \frac{h}{R_{\text{opt}}} = \frac{h}{n\rho}, \quad (2.58)$$

which may be recognised as Snell's law for a radially-stratified medium.

For a geodesic that spirals around a photon sphere or an anti-photon sphere we have from (2.53) that $h = R_{\text{opt}}(\bar{r})$, whence for such geodesics

$$\sin \delta(r) = \frac{R_{\text{opt}}(\bar{r})}{R_{\text{opt}}(r)}. \quad (2.59)$$

If $r > \bar{r}_{\text{max}}$, where \bar{r}_{max} is the position of the outermost photon sphere, then (2.59) gives the angle subtended by the shadow cast by this photon sphere [11]. For the Kottler metric one has

$$\sin \delta = \frac{3M}{R} \frac{\sqrt{1 - \frac{2M}{R} - \frac{1}{3}\Lambda R^2}}{\sqrt{\frac{1}{3} - 3\Lambda M^2}}, \quad (2.60)$$

and so $\delta = \frac{\pi}{2}$ at $R = 3M$ (the photon sphere), independently of Λ as expected. However the variation of δ with radius definitely does depend upon Λ , since it is not a projectively invariant observable [15, 31].

2.4.3 Cross sections and quasi-normal modes

If the metric is asymptotically flat then $R_{\text{opt}}(\bar{r}_{\text{max}})$ is the critical impact parameter such that light rays with smaller impact parameter cannot return to infinity. Thus the high-energy limit of the absorption cross section is given by

$$\sigma = \pi R_{\text{opt}}^2(\bar{r}_{\text{max}}). \quad (2.61)$$

For the Schwarzschild solution, the photon sphere is at $R = 3M$ and thus

$$R_{\text{opt}}(\bar{r}_{\text{max}}) = \sqrt{27}M, \quad \sigma = 27\pi M^2. \quad (2.62)$$

Modes of oscillation of fields around black holes can become trapped near photon spheres, and give rise to long-lived quasi-normal modes [12]. Following [13], one may estimate that in the large l limit, the real part of the frequency behaves like

$$\omega \approx \frac{l + \frac{1}{2}}{R_{\text{opt}}(\bar{r}_{\text{min}})}. \quad (2.63)$$

2.5 York-Hawking-Page phase transition

We conclude this brief review of the physics of photon spheres by noting its connection with the York-Hawking-Page phase transition. The York-Hawking-Page phase transition [4–6] plays a role when we wish to count solutions of the Dirichlet problem for the Riemannian Einstein equations [4, 7]. The geometries must be matched properly at the boundary. Thus, in the spherically symmetric case we must match the circumference C_β (or the local inverse temperature) of the $U(1)$ thermal circle, and the circumference C_S of the boundary sphere which we assume to be situated at $R = R_b$. Now

$$C_\beta = \frac{2\pi}{\kappa} e^{U(R_b)}, \quad (2.64)$$

and

$$C_S = 2\pi R_b \quad (2.65)$$

where κ , the surface gravity, is a function of the parameters defining the solution. For example for the Kottler solution

$$e^{2U} = \left(1 - \frac{2M_{AD}}{R} + g^2 R^2\right), \quad (2.66)$$

where M_{AD} is the Abbot-Deser mass, $g^2 = -\frac{\Lambda}{3}$, and $\kappa = \kappa(M_{AD}, g)$ is given by eliminating r_H from the equations

$$\frac{M_{AD}}{R_H^2} + g^2 R_H = \kappa \quad (2.67)$$

$$1 - \frac{2M_{AD}}{R_H} + g^2 R_H^2 = 0. \quad (2.68)$$

Thus any saddle point of the path integral must satisfy

$$\frac{\kappa C_S}{C_\beta} = R_{\text{opt}}(R_b), \quad (2.69)$$

where $R_{\text{opt}}(R_b)$ is the optical radius of the boundary. If we plot the graph of R_{opt} against R_b , the allowed values of r_b correspond to the intersection of the curve with the horizontal line determined by the left-hand side of (2.69).

As the left-hand side of (2.69) varies, solutions will appear or disappear in pairs, at values of R_b for which

$$\frac{dR_{\text{opt}}}{dR_b} = 0. \quad (2.70)$$

That is, the number of solutions will jump when the boundary is a photon or an anti-photon sphere..

Naively these values correspond to phase transitions. More accurately, they signal jumps in the minimum values of the Helmholtz free energy of the system. *It is a general feature that the location of the boundary values R_b for which the saddle points jump in number is independent of the cosmological constant.*

3 Static Spherically Symmetric STU Black Holes in Four Dimensions

In this section we shall explore in detail properties of photon spheres for static black holes in four dimensional (gauged) supergravity theories. The prototypes are black holes of maximally supersymmetric (gauged) supergravity theory, supported by four Abelian gauge potentials and three scalar axion-dilaton pairs. These fields in fact comprise a consistent truncation of the maximal gauged supergravity to the $N = 2$ supersymmetric gauged STU supergravity theory. Furthermore, since we are focusing solely on static solutions, only the three dilaton fields and the four electric gauge potentials are turned on.

3.1 Static four-charge STU black holes

For the static spherically-symmetric solutions of the (maximally supersymmetric) STU gauged supergravity the black-hole metrics are given by [32, 33]

$$ds^2 = -(H_1 H_2 H_3 H_4)^{-\frac{1}{2}} f dt^2 + (H_1 H_2 H_3 H_4)^{\frac{1}{2}} \left[\frac{dr^2}{f} + r^2 d\Omega_2^2 \right], \quad (3.1)$$

with

$$f = 1 - \frac{2m}{r} + g^2 r^2 H_1 H_2 H_3 H_4, \quad (3.2)$$

and the harmonic functions H_i are given by

$$H_i = 1 + \frac{q_i}{r}, \quad i = 1, 2, 3, 4. \quad (3.3)$$

The ADM mass and the physical charges are determined in terms of m and q_i as:

$$M_{ADM} = \sum_{i=1}^4 M_i, \quad M_i = \frac{1}{4}(m + q_i), \quad Q_i^2 = q_i(q_i + 2m), \quad i = 1, 2, 3, 4. \quad (3.4)$$

For $m \geq 0$ and $q_i = 2m \sinh^2 \delta_i \geq 0$, the solutions have a regular horizon, and

$$M_{ADM} = \frac{1}{4}m \sum_{i=1}^4 (\sinh^2 \delta_i + \cosh^2 \delta_i) \geq 0, \quad Q_i = 2m \sinh \delta_i \cosh \delta_i \geq 0. \quad (3.5)$$

The solution can be uniquely parameterized in terms of physical charges Q_i , chosen, without loss of generality, to be positive, and the positive ADM mass M_{ADM} , satisfying a BPS bound (of $N = 8$ supergravity):

$$M_{ADM} \geq \frac{1}{4} \sum_{i=1}^4 Q_i. \quad (3.6)$$

We shall refer to these solutions as non-extremal ones.

If any of the $q_i \equiv -p_i$ parameters is chosen to be negative, the solution has a naked singularity at $r = p_{i\max}$. These solutions have mass below the BPS bound, and we shall refer to them as “ultra-extremal.” Note from the expression for Q_i^2 in (3.4) that we must have $p_i \geq 2m$ in order that Q_i be real.

Isotropic coordinates and index of refraction

In [34], the static non-extremal STU black holes of the ungauged supergravity ($g^2 = 0$) [35, 36] were re-written in terms of isotropic coordinates. Defining an isotropic radial coordinate ρ by $r = \rho + m + \frac{m^2}{4\rho}$, it follows that

$$\frac{dr^2}{1 - \frac{2m}{r}} + r^2(d\theta^2 + \sin^2\theta d\phi^2) = \left(1 + \frac{m}{2\rho}\right)^4 \{d\rho^2 + \rho^2 d\Omega^2\}. \quad (3.7)$$

It now follows that

$$\left(1 + \frac{m}{2\rho}\right)^2 H_i = C_i D_i, \quad (3.8)$$

where C_i and D_i are spherically-symmetric harmonic functions:

$$C_i = 1 + \frac{me^{2\delta_i}}{2\rho}, \quad D_i = 1 + \frac{me^{-2\delta_i}}{2\rho}. \quad (3.9)$$

Note that C_i and D_i , unlike the functions H_i themselves, are harmonic in the flat transverse 3-metric $d\rho^2 + \rho^2 d\Omega^2$.

In terms of the isotropic radial coordinate, the metric (3.1) becomes

$$ds^2 = -\Pi^{-1/2} f_+^2 f_-^2 dt^2 + \Pi^{1/2} (d\rho^2 + \rho^2 d\Omega^2), \quad (3.10)$$

where we have defined

$$\Pi = \prod_{1 \leq I \leq 4} C_I D_I, \quad f_{\pm} = 1 \pm \frac{m}{2\rho}. \quad (3.11)$$

The scalar fields and gauge potentials can be written as

$$X_i = \frac{\Pi^{1/4}}{C_i D_i}, \quad A_{\mu}^i dx^{\mu} = \left(-\frac{1}{C_i} + \frac{1}{D_i}\right) dt. \quad (3.12)$$

Here we also provide the explicit parameterisation for ultra-extremal solutions with one or more $q_i \equiv -p_i \leq 0$. For $m > 0$, the condition $Q_i^2 \geq 0$ on the charges implies that $p_i \geq 2m$. The metric still takes the form (3.10), with the harmonic functions written as:

$$C_i = 1 + \frac{\alpha_i}{2\rho} \quad D_i = 1 + \frac{\beta_i}{2\rho}, \quad (3.13)$$

where

$$\alpha_i = m + q_i + \sqrt{(m + q_i)^2 - m^2}, \quad \beta_i = m + q_i - \sqrt{(m + q_i)^2 - m^2}. \quad (3.14)$$

Note that these harmonic functions are well defined both for $q_i \geq 0$ (and reduce for $q_i = 2m \sinh^2 \delta_i$ to (3.9)), as well as for $q_i \equiv -p_i$, as long as $p_i \geq 2m$. Again, the latter case corresponds to ultra-extremal solutions with a naked singularity at $\rho = -\frac{\beta_i}{2}$.

Note that the index of refraction is simply obtained from the form (3.10) as:

$$n(\rho) = \frac{\Pi^{\frac{1}{2}}}{f_+ f_-}. \quad (3.15)$$

While the index of refraction for non-extremal solutions blows-up at the outer horizon $\rho = \frac{m}{2}$, for the ultra-extremal solutions it blows-up at the naked singularity $\rho = -\frac{\beta_i}{2}$.

3.2 Photon spheres

In this subsection we analyse the properties of the photon spheres for these metrics. The radius of the photon sphere is simply determined from (3.1) as:

$$\frac{1}{R_{\text{opt}}^2} = \frac{1}{r^2 H_1 H_2 H_3 H_4} \left(1 - \frac{2m}{r}\right) + g^2. \quad (3.16)$$

As argued in Section 2, one may note that the existence and location of any circular geodesic $r_{\star \text{min}}$ or $r_{\star \text{max}}$ is independent of g^2 , but the optical radius of any photon $R_{\text{opt}}(r_{\star \text{min}})$ or anti-photon surface $R_{\text{opt}}(r_{\star \text{max}})$ will depend upon g^2 , as do the quasi-normal modes, and also the angle of any shadow. In the present case, the optical circumference is an extremum when

$$\frac{2(r - 3m)}{(r - 2m)} = \sum_{i=1}^4 \frac{q_i}{(r + q_i)}. \quad (3.17)$$

Non-extremal solutions

The non-extremal solutions are parameterized by the positive quantity m and the four positive quantities $q_i = 2m \sinh^2 \delta_i \geq 0$. By analysing (3.17), it is straightforward to show that outside the outer horizon at $r = r_+$, there is only one extremum, which is located at $r = \bar{r} > 3m$.³ Namely, the left-hand side of (3.17) is a monotonically-increasing function of r , with a negative pole at $r \rightarrow 2m^+$, zero at $r = 3m$ and approaching 2 as $r \rightarrow \infty$. On the other hand, the right-hand side is a monotonically-decreasing function of r , with a positive finite value at $r = 2m$ and approaching 0 as $r \rightarrow \infty$. Thus there is only *one* common solution in this domain, at $r = \bar{r} > 3m$. It is straightforward to show that the extremum is a *minimum*, and so it gives a single unstable circular null geodesic.

³For $g^2 = 0$, $r_+ = 2m$, and for $g^2 > 0$, $r_+ < 2m$. and thus the result of the analysis above applies to both cases.

In the following we shall also address the theorem (2.45) and the conjecture (2.50) of Hod [8, 9].

We can also show that for the case of fewer than two charges turned on, the conjecture (2.50) of Hod [8] is violated. For concreteness we take only $q_1 = q_2 \neq 0$. In this case we have the ratio

$$\frac{R_{\text{opt}}(\bar{r})^2}{4M_{ADM}^2} = \frac{1}{16} \frac{(3 + \sqrt{8\tilde{q} + 9} + 4\tilde{q})^2 (3 + \sqrt{8\tilde{q} + 9})}{(-1 + \sqrt{8\tilde{q} + 9}) (\tilde{q} + 1)^2} \geq 1, \quad (3.18)$$

where $\tilde{q} \equiv \frac{q}{2m}$. The equality is attained in the limit $\delta \rightarrow \infty$. The analysis of the single charge case (e.g. only $q_1 \neq 0$) reveals that the conjecture is violated when $\tilde{q}_1 \equiv \frac{q_1}{2m} \geq 13.94$.

It is straightforward to show that Hod's theorem [9], given in (2.45), is satisfied. Namely, one can write

$$\bar{R} = \prod_{i=1}^4 (\bar{r} + q_i)^{\frac{1}{4}} \leq \frac{1}{4} \sum_{i=1}^4 (\bar{r} + q_i) = 3M_{ADM} + \bar{r} - 3m - \frac{1}{2} \sum_{i=1}^4 q_i \leq 3M_{ADM}. \quad (3.19)$$

The first inequality above is due to the inequality of geometric and arithmetic means. The second inequality is due to the fact that:

$$\bar{r} - 3m - \frac{1}{2} \sum_{i=1}^4 q_i = -\frac{1}{2} \sum_{i=1}^4 \frac{q_i(q_i + 2m)}{\bar{r} + q_i} \leq 0. \quad (3.20)$$

where where the first equality is due to (3.17).

One can also show that the inequality in Hod's theorem (2.47) is also satisfied.

Ultra-extremal solutions

The occurrence of photon spheres in extremal black holes has been extensively studied, for example in [37, 38], and we shall not consider this case further here. Instead, we move on to a study of the ultra-extremal case, where one or more of the q_i parameters is negative. For $q_i \equiv -p_i$, with $p_i \geq 2m$ and $i = 1, \dots, k$, the extremum equation for the photon radius takes the form:

$$\frac{2(r - 3m)}{(r - 2m)} = \sum_{i=1}^k \frac{-p_i}{(r - p_i)} + \sum_{j=k+1}^4 \frac{q_j}{(r + q_j)}. \quad (3.21)$$

A straightforward analysis shows that a necessary condition for the above equation to have a solution is that $k = 1$, i.e. only one of the q_i is negative. To see this, we take $q_1 = -p_{max}$ and $k \geq 2$, so Eq. (3.21) can be written as:

$$2 + \frac{r(p_{max} - 2m)}{(r - 2m)(r - p_{max})} + \sum_{i=2}^k \frac{p_i}{(r - p_i)} = \sum_{j=k+1}^4 \frac{q_j}{(r + q_j)}, \quad (3.22)$$

where the p_i for $i \geq 2$ satisfy $p_i \leq p_{max}$. The naked singularity is located at $r = p_{max}$. The left-hand side of (3.22) is manifestly larger than 2 for $r \geq p_{max}$. The necessary condition

for the solution to exist is that the right-hand side of (3.22) be ≥ 2 for $r = p_{max}$. This condition cannot be satisfied for $k \geq 2$, thus demonstrating that photon spheres can arise for ultra-extremal black holes only if just a single q_i is negative.

For $k = 1$, the left-hand side of (3.22) lacks the final term, and it remains ≥ 2 for $r \geq p_{max}$. In this case the necessary condition that the right-hand side be ≥ 2 for $r = p_{max}$ reduces to the condition

$$\prod_{i=2}^4 \frac{q_i}{p_{max}} \geq \sum_{i=2}^4 \frac{q_i}{p_{max}} + 2, \quad (3.23)$$

which can be satisfied for a range of parameters q_i . For the case $q_2 = q_3 = q_4 \equiv q$, the above inequality is satisfied for $q \geq 2p_{max}$.

Further focusing on the latter case, namely, $q_1 \equiv -p$ and $q_2 = q_3 = q_4 \equiv q$, eqn (3.22) becomes

$$2 + \frac{\tilde{r}(\tilde{p} - 1)}{(\tilde{r} - 1)(\tilde{r} - \tilde{p})} = \frac{3\tilde{q}}{(\tilde{r} + \tilde{q})}, \quad (3.24)$$

where we have defined

$$\tilde{r} \equiv \frac{r}{2m}, \quad \tilde{q} = \frac{q}{2m}, \quad \tilde{p} \equiv \frac{p}{2m}. \quad (3.25)$$

Plotting the left and right hand sides one can see that there will be either two intersections or none, in the region $\tilde{r} > \tilde{p}$ outside the naked singularity, depending on the choice of the parameters. The critical intermediate case occurs if the parameters are such that the left and right hand sides, and also their first derivatives, are equal for some \tilde{r}_{crit} . These two conditions allow one to derive the corresponding values of \tilde{p}_{crit} and \tilde{r}_{crit} in terms of \tilde{q} . The result is

$$\begin{aligned} \tilde{r}_{crit} &= \frac{1}{2} \left(4\tilde{q} + 3 - \sqrt{12\tilde{q}^2 + 12\tilde{q} + 9} \right), \\ \tilde{p}_{crit} &= \frac{(26\tilde{q}^2 + 27\tilde{q} + 9)\sqrt{12\tilde{q}^2 + 12\tilde{q} + 9} - 90\tilde{q}^3 - 138\tilde{q}^2 - 99\tilde{q} - 27}{(2\tilde{q} + 1)\sqrt{12\tilde{q}^2 + 12\tilde{q} + 9} - 6\tilde{q}^2 - 6\tilde{q} - 3}. \end{aligned} \quad (3.26)$$

It is straightforward to show that $2m \leq p_{crit} \leq \frac{1}{2}q$, and $r_{crit} \geq p_{crit}$, i.e., the extremum is located outside the naked singularity.

In summary, we have shown that for $p \geq p_{crit}$, Eq. (3.21) has no solution, whilst for $p \leq p_{crit}$, Eq. (3.21) has two solutions. In the latter case, the outer solution corresponds to a minimum, which is stable (an anti-photon sphere) and the inner solution to a maximum, which is therefore unstable (a photon sphere).

3.3 Projective symmetry for the general STU black holes

The optical metric of a static black hole can always be cast in the form

$$\frac{du^2}{k^2(u)} + \frac{1}{k(u)} d\Omega_2^2. \quad (3.27)$$

It was shown in [15] that the Weyl projective tensor depends only on k' and k'' . For metrics of the form (3.27), one can assume that coordinates may be chosen so that any geodesic lies in the equatorial plane $\theta = \frac{\pi}{2}$. The geodesics then satisfy

$$\left(\frac{du}{d\phi}\right)^2 + k = \frac{1}{h^2} \quad (3.28)$$

where h is Clairaut's constant, which may be thought of as the angular momentum or impact parameter. Differentiating (3.28) we obtain the second-order equation

$$\frac{d^2u}{d\phi^2} + \frac{1}{2}k' = 0. \quad (3.29)$$

The optical metric of the static STU black hole (3.1) can be cast in the form (3.27), by introducing a coordinate $u = u(r)$ such that

$$k(u) = \frac{f}{r^2 H}, \quad \frac{u'^2 f^2}{H} = k^2(u), \quad (3.30)$$

where $H \equiv \prod_{i=1}^4 H_i(r)$ and $H_i(r)$ and $f(r)$ are defined in Eq. (3.1). This implies that u is given by

$$u = \int^r \frac{dr'}{\prod_i (r' + q_i)^{\frac{1}{2}}}. \quad (3.31)$$

This integral can be evaluated, to give

$$u = \frac{2}{(q_2 - q_3)^{\frac{1}{2}} (q_1 - q_4)^{\frac{1}{2}}} F\left(\frac{(q_1 - q_4)^{\frac{1}{2}} (r + q_2)^{\frac{1}{2}}}{(q_2 - q_4)^{\frac{1}{2}} (r + q_1)^{\frac{1}{2}}}; \frac{(q_1 - q_3)^{\frac{1}{2}} (q_2 - q_4)^{\frac{1}{2}}}{(q_2 - q_3)^{\frac{1}{2}} (q_1 - q_4)^{\frac{1}{2}}}\right), \quad (3.32)$$

where the incomplete elliptic function of the first kind is defined by

$$F(\sin \varphi; \kappa) = \int_0^\varphi \frac{d\theta}{\sqrt{1 - \kappa^2 \sin^2 \theta}}. \quad (3.33)$$

Note that the function $k(u)$, defined by the first equation in (3.30), is given by

$$k(u) = \frac{1}{R_{\text{opt}}^2} = \frac{1}{r^2 H} \left(1 - \frac{2m}{r}\right) + g^2, \quad (3.34)$$

where u is defined in terms of r by (3.32), and thus the projective symmetry condition is satisfied (since $k'(u)$ is independent of g^2). The expression for r in terms of u can be made explicit in terms of the Jacobi elliptic function $\text{sn}(v; \tilde{k})$, which is related to the incomplete elliptic integral by $F(x; \tilde{k}) = v$, where $x = \text{sn}(v; \tilde{k})$. Thus we find

$$r = \frac{q_1(q_2 - q_4) \text{sn}^2(v; \tilde{k}) - q_2(q_1 - q_4)}{(q_1 - q_4) - (q_2 - q_4) \text{sn}^2(v; \tilde{k})}, \quad (3.35)$$

where

$$v = \frac{1}{2}(q_2 - q_3)^{\frac{1}{2}} (q_1 - q_4)^{\frac{1}{2}} u, \quad \tilde{k} = \frac{(q_1 - q_3)^{\frac{1}{2}} (q_2 - q_4)^{\frac{1}{2}}}{(q_2 - q_3)^{\frac{1}{2}} (q_1 - q_4)^{\frac{1}{2}}}. \quad (3.36)$$

For the special case of pair-wise equal charges $q_1 = q_3$ and $q_2 = q_4$, the transformation is invertible in terms of elementary functions:

$$u = \frac{1}{q_2 - q_1} \log\left(\frac{r + q_2}{r + q_1}\right), \quad (3.37)$$

and

$$r = \frac{q_1 x - q_2}{1 - x}, \quad x = \exp((q_2 - q_1)u). \quad (3.38)$$

For the Reissner-Nordström case $q_1 = q_2 = q_3 = q_4 \equiv q$, the relation between u and r is very simple, namely

$$u = \frac{1}{r + q}. \quad (3.39)$$

In this case $u = \frac{1}{R}$, where R is the area distance. It is easy to check that the geodesics of the optical metric are given by Weierstrass functions of the azimuthal coordinate ϕ in this case (c.f. [48]). Setting $q = 0$ and we recover the Schwarzschild case [49].

In general case one may define $\tilde{u} = \frac{1}{r}$ and obtain the equation

$$\left(\frac{d\tilde{u}}{d\phi}\right)^2 + \tilde{u}^2 - 2m^3 + \left(g^2 - \frac{1}{h^2}\right)H(\tilde{u}) = 0. \quad (3.40)$$

It follows that the geodesics of the optical metric are given in general by Weierstrass functions of the azimuthal coordinate ϕ .

One may also evaluate the Weyl projective tensor directly in the r coordinates and verify that it does not depend on g^2 .

3.4 Dyonic solutions of the gauged STU model

Here we show that analogous properties of the STU black holes also hold for the case of the dyonic black hole solutions found in [39]. These black holes are solutions of the theory described by the Lagrangian

$$\mathcal{L} = \sqrt{-g} \left[R - \frac{1}{2}(\partial\phi)^2 - \frac{1}{2}e^{-\sqrt{3}\phi} F^2 + 6g^2 \cosh\left(\frac{1}{\sqrt{3}}\phi\right) \right]. \quad (3.41)$$

This theory is the bosonic sector of a consistent truncation of $\mathcal{N} = 8$ gauged supergravity in which just a single $U(1)$ gauge field is retained. It is also a consistent truncation of gauged STU supergravity. The dyonic black hole solution is given by [39]

$$ds^2 = -(H_1 H_2)^{-\frac{1}{2}} f dt^2 + (H_1 H_2)^{\frac{1}{2}} \left(\frac{dr^2}{f} + r^2 d\theta^2 + r^2 \sin^2 \theta d\varphi^2 \right), \quad (3.42)$$

where

$$\begin{aligned} \phi &= \frac{\sqrt{3}}{2} \log \frac{H_2}{H_1}, & f &= f_0 + g^2 r^2 H_1 H_2, & f_0 &= 1 - \frac{2m}{r}, \\ A &= \sqrt{2} \left(\frac{1 - \beta_1 f_0}{\sqrt{\beta_1 \gamma_2} H_1} dt + 2m \gamma_2^{-1} \sqrt{\beta_2 \gamma_1} \cos \theta d\varphi \right), \\ H_1 &= \gamma_1^{-1} (1 - 2\beta_1 f_0 + \beta_1 \beta_2 f_0^2), & H_2 &= \gamma_2^{-1} (1 - 2\beta_2 f_0 + \beta_1 \beta_2 f_0^2). \end{aligned} \quad (3.43)$$

The constants m , β_1 and β_2 characterise the mass, electric and magnetic charges [39], and the constants γ_1 and γ_2 are given in terms of β_1 and β_2 by

$$\gamma_1 = 1 - 2\beta_1 + \beta_1\beta_2, \quad \gamma_2 = 1 - 2\beta_2 + \beta_1\beta_2. \quad (3.44)$$

The constants β_1 and β_2 , which must each lie in the range $0 \leq \beta_i \leq 1$, are further constrained by the requirement, for positivity of the functions H_i , that $\gamma_i \geq 0$.

The radius of the extremal photon sphere satisfies

$$\frac{2(r - 3m)}{(r - 2m)} = -r \left(\frac{H'_1}{H_1} + \frac{H'_2}{H_2} \right), \quad (3.45)$$

where $H'_i \equiv \frac{dH_i}{dr}$. It is straightforward to show that

$$-r H'_1 = \frac{2\beta_1 [1 + x(1 - \beta_2)]}{(1 + x)^2} \geq 0, \quad (3.46)$$

where $r = 2m(1 + x)$, with an analogous result for H'_2 in which the labels 1 and 2 are interchanged. Since $r \geq 2m$ corresponds to $x \geq 0$, it is manifest that the right-hand side of (3.45) is always non-negative for $x \geq 0$ (i.e. $r \geq 2m$). It approaches the value $2(\beta_1 + \beta_2)$ as x goes to zero, and it goes to zero as x goes to infinity.

Furthermore, one can see that the right-hand side of (3.45) is a monotonically decreasing function of x . Namely, one can show that

$$\left(-r \frac{H'_1}{H_1} \right)' = -\frac{\beta_1}{m H_1^2} \left[\gamma_1 + \beta_2(1 - \beta_1) + 2x\gamma_1 + x^2\gamma_1(1 - \beta_2) \right] \leq 0, \quad (3.47)$$

with an analogous result where the labels 1 and 2 are interchanged. Thus there is only one solution of (3.45), at $r = \bar{r} \geq 3m$, just as in the 4-charge solution of section 3.1.

4 Einstein-Maxwell-Dilaton Black Holes

In this section, we study the properties of photon spheres for static black holes in the family of Einstein-Maxwell-Dilaton (EMD) theories.

4.1 Static black holes in EMD theories

Einstein-Maxwell-Dilaton gravity is described by the Lagrangian

$$\mathcal{L} = \sqrt{-g} (R - 2(\partial\phi)^2 - e^{-2a\phi} F^2). \quad (4.1)$$

The static black hole solution is given by [40]

$$ds^2 = -\Delta dt^2 + \Delta^{-1} dr^2 + R^2 d\Omega_2^2,$$

$$\begin{aligned}
e^{-2a\phi} &= F_-^{\frac{2a^2}{1+a^2}}, & A &= Q \cos \theta d\varphi, \\
\Delta &= F_+ F_-^{\frac{(1-a^2)}{(1+a^2)}}, & R^2 &= r^2 F_-^{\frac{2a^2}{(1+a^2)}}, \\
F_{\pm} &= 1 - \frac{r_{\pm}}{r},
\end{aligned} \tag{4.2}$$

and

$$M_{ADM} = \frac{1}{2} \left(r_+ + \frac{1-a^2}{1+a^2} r_- \right), \quad Q^2 = \frac{r_+ r_-}{1+a^2}. \tag{4.3}$$

If a potential of the type considered in [41] is added, namely

$$V(\phi) = -\frac{2\lambda}{3(1+a^2)^2} \left[a^2(3a^2-1)e^{-\frac{2\phi}{a}} + (3-a^2)e^{2a\phi} + 8a^2e^{(a\phi-\frac{\phi}{a})} \right], \tag{4.4}$$

the only change to the solution is in the function Δ , which is then given by [41]

$$\Delta = F_+ F_-^{\frac{1-a^2}{1+a^2}} - \frac{\lambda}{3} R^2. \tag{4.5}$$

4.1.1 Isotropic coordinates and refractive index

If $\lambda = 0$, we can introduce an isotropic radial coordinate ρ , defined by

$$\log \rho = \int \frac{1}{r \sqrt{F_- F_+}} dr, \tag{4.6}$$

which implies that, with a convenient choice for the constant of integration,

$$r = \rho \left(1 + \frac{u^2}{\rho} \right) \left(1 + \frac{v^2}{\rho} \right), \tag{4.7}$$

where we have re-parameterised the constants r_{\pm} in terms of constants u and v as

$$r_+ = (u+v)^2, \quad r_- = (u-v)^2. \tag{4.8}$$

In terms of the new quantities, we have

$$F_- = \frac{\left(1 + \frac{uv}{\rho} \right)^2}{\left(1 + \frac{u^2}{\rho} \right) \left(1 + \frac{v^2}{\rho} \right)}, \quad F_+ = \frac{\left(1 - \frac{uv}{\rho} \right)^2}{\left(1 + \frac{u^2}{\rho} \right) \left(1 + \frac{v^2}{\rho} \right)}. \tag{4.9}$$

The metric now takes the form

$$ds^2 = -\Delta dt^2 + \Phi^4 (d\rho^2 + \rho^2 d\Omega_2^2), \tag{4.10}$$

where

$$\Phi^2 = \frac{R}{\rho} = \left[\left(1 + \frac{u^2}{\rho} \right) \left(1 + \frac{v^2}{\rho} \right) \right]^{\frac{1}{1+a^2}} \left(1 + \frac{uv}{\rho} \right)^{\frac{2a^2}{1+a^2}}, \tag{4.11}$$

and with the dilaton given by

$$e^{2a\phi} = \left[\left(1 + \frac{u^2}{\rho} \right) \left(1 + \frac{v^2}{\rho} \right) \right]^{-\frac{2a^2}{1+a^2}} \left(1 + \frac{uv}{\rho} \right)^{\frac{4a^2}{1+a^2}}. \tag{4.12}$$

The effective refractive index $n(\rho)$ in this representation is given by

$$n(\rho) = \frac{\Phi^2(\rho)}{\sqrt{\Delta(\rho)}} = \frac{\left[\left(1 + \frac{u^2}{r}\right) \left(1 + \frac{v^2}{r}\right) \right]^{\frac{3}{1+a^2}}}{\left(1 + \frac{uv}{r}\right)^{\frac{2}{1+a^2}} \left(1 - \frac{uv}{r}\right)^{\frac{2(1-a^2)}{1+a^2}}}. \quad (4.13)$$

4.2 Photon spheres and Hod's conjecture

For the static dilatonic black holes solutions [41], discussed above, the photon radius is of the form:

$$\frac{1}{R_{\text{opt}}^2} = \frac{1}{r^2} F_+ F_-^{\frac{1-3a^2}{1+a^2}} - \frac{1}{3} \lambda. \quad (4.14)$$

Thus the independence of the location of the photon spheres on the cosmological constant continues to hold in this case as well. The extremal values of the photon spheres are at values of $r = \bar{r}$ satisfying the equation

$$\frac{3}{r} - \frac{1}{r - r_+} + \frac{3a^2 - 1}{1 + a^2} \frac{r_-}{r} \frac{1}{r - r_-} = 0. \quad (4.15)$$

This quadratic equation determines two stationary points, $r = b_{\pm}$, with

$$b_{\pm} = \frac{1}{4} \left[3r_+ + (2 - x)r_- \pm \sqrt{[(2 - x)r_- - r_+]^2 + 8r_+(r_+ - r_-)} \right], \quad (4.16)$$

where $x \equiv (3a^2 - 1)/(a^2 + 1)$. Noting that $1 + x = 4a^2/(a^2 + 1) \geq 0$ and $3 - x = 4/(a^2 + 1) \geq 0$, it follows that x lies in the range $-1 \leq x \leq 3$. Assuming $0 \leq r_- \leq r_+$ we have $\sqrt{[(2 - x)r_- - r_+]^2 + 8r_+(r_+ - r_-)} \geq |Z|$, where we define

$$Z = (2 - x)r_- - r_+ \quad (4.17)$$

(which may have either sign). It then follows that

$$b_+ - r_+ \geq \frac{1}{4}(Z + |Z|) \geq 0, \quad b_- - r_+ \leq \frac{1}{4}(Z - |Z|) \leq 0, \quad (4.18)$$

and so the larger stationary point always lies outside the outer horizon, while the smaller stationary point lies inside.

4.2.1 Photon spheres: Non-extremal dilatonic solutions

In [9], Hod conjectured the bound (2.50) for static black holes, or, in other words,

$$\mathcal{N} \equiv \frac{R_{\text{opt}}(\bar{r})^2}{4M_{\text{ADM}}^2} \geq 1, \quad (4.19)$$

For the dilatonic black holes with $\lambda = 0$, it is straightforward to show that this bound is satisfied when $a^2 \leq 1$ for any value of the ratio $\frac{r_-}{r_+} \leq 1$. At a critical value $a^2 = 1$, we have $\mathcal{N} = 1$ for $\frac{r_-}{r_+} = 1$. For $a^2 > 1$ the bound is violated, i.e., $\mathcal{N} < 1$ for sufficiently large

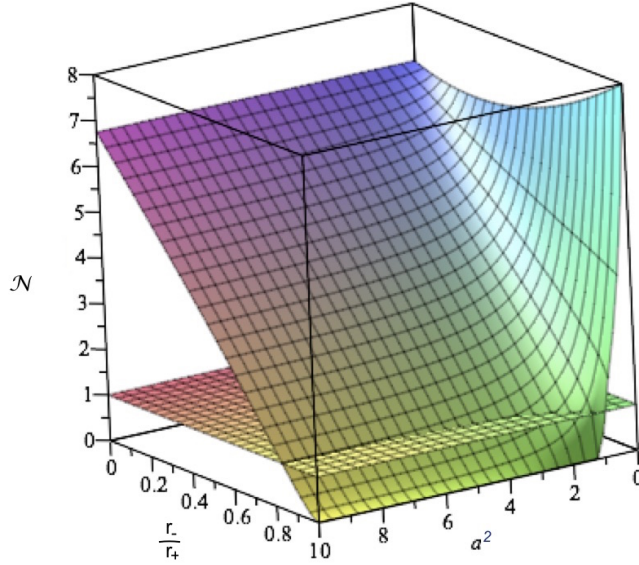


Figure 1: The ratio $\mathcal{N} = \frac{R_{\text{opt}}(\bar{r})^2}{4M_{ADM}^2}$ as a function of $\frac{r_-}{r_+}$ and a^2 .

values of the ratio $\frac{r_-}{r_+}$. In the limiting case of large a^2 , the bound is violated for $0.85 \lesssim \frac{r_-}{r_+}$. These features are quantitatively displayed in Figure 1, which depicts the value of \mathcal{N} as a function of $\frac{r_-}{r_+}$ and a^2 . The figure further confirms that \mathcal{N} is bounded from above by 8, and that it saturates this bound for the extremal Reissner-Nordström black hole:

$$R_{\text{opt}}(\bar{r}) \leq 4\sqrt{2} M_{ADM}. \quad (4.20)$$

This bound is saturated for the extremal Reissner-Nordström black hole.

Hod's theorem (2.45) states that

$$R(\bar{r}) = R_{\text{opt}}(\bar{r}) (-g_{tt}(\bar{r}))^{\frac{1}{2}} \leq 3M_{ADM}. \quad (4.21)$$

This is clearly satisfied, since both $R_{\text{opt}}(\bar{r})$ and $|g_{tt}(\bar{r})|$ are bounded from below. The bound is saturated when the ratio $\frac{r_-}{r_+}$ goes to zero. We illustrate these results in Figure 2.

4.2.2 Photon spheres for ultra-extremal dilatonic solutions

We now turn to the analysis of photon spheres in the case when the solutions have a mass below the BPS bound, i.e. ultra-extremal black holes. It is convenient parameterise r_{\pm} in terms of the charge and the ADM mass of the black holes:

$$\begin{aligned} r_+ &= M_{ADM} + \sqrt{M_{ADM}^2 - (1 - a^2)Q^2}, \\ r_- &= \frac{1 - a^2}{1 + a^2} \left(M_{ADM} - \sqrt{M_{ADM}^2 - (1 - a^2)Q^2} \right). \end{aligned} \quad (4.22)$$

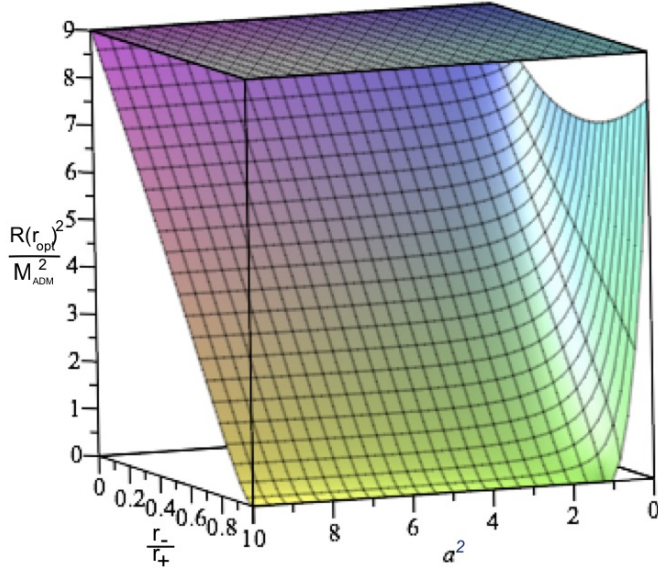


Figure 2: The ratio of $\frac{R(\bar{r})^2}{M_{ADM}^2}$ is plotted as a function of $\frac{r_-}{r_+}$ and a^2 . Note the ratio is always smaller than 9, thus confirming the bound.

The extremal black hole with the property $r_+ = r_-$ saturates the BPS bound:

$$M_{ADM}^2 = \frac{Q^2}{1 + a^2}, \quad (4.23)$$

Note that for $a^2 \leq 1$, there is a range of ultra-extremal black holes with

$$\frac{Q^2}{1 + a^2} \geq M_{ADM}^2 \geq (1 - a^2)Q^2. \quad (4.24)$$

In this regime, $\frac{r_-}{r_+} \geq 1$, namely, the outer horizon is at r_- and the inner one at r_+ . From the analysis of the extremal equation of the photon sphere it is now possible to show that for $\frac{1}{3} \leq a^2 \leq 1$, *both* extrema of the photon sphere (4.16) lie *outside* the larger horizon r_- , as long as

$$1 \leq \frac{r_-}{r_+} \leq \frac{9(a^2 + 1)}{3a^2 + 7 + 4\sqrt{2(3a^2 - 1)}}, \quad (4.25)$$

For a^2 in the range $\{\frac{1}{3}, 1\}$, the upper bound in (4.25) has the range $\{\frac{3}{2}, 1\}$. We illustrate these results in Figure 3. In this range of parameters the outer photon radius corresponds to a minimum, which is stable (an anti-photon sphere), and the inner solution to a maximum, which is therefore unstable (a photon sphere).

4.3 Projective symmetry for the dilatonic black holes

Here we demonstrate that the static dilatonic black holes also exhibit the projective symmetry, just as we demonstrated for the static STU black holes in Subsection 3.3.

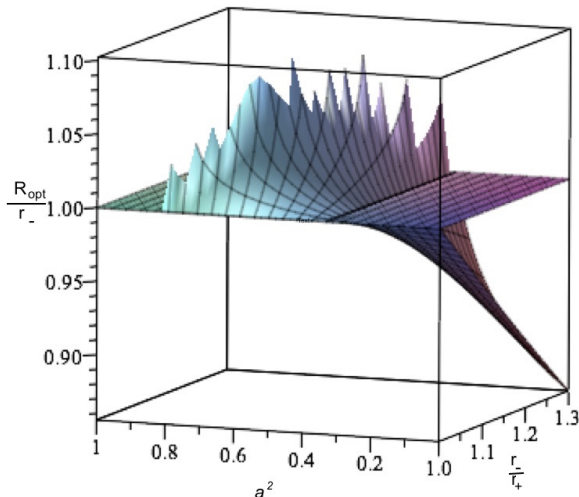


Figure 3: The range of the second extremal photon radius plotted for $\frac{R_{\text{opt}}(\bar{r})}{r_-}$ as a function of $\frac{r_-}{r_+} \geq 1$ (ultra extremal solutions) and a^2 . Note that for $a^2 \geq \frac{1}{3}$, there is always a range of $\frac{r_-}{r_+} > 1$ for which the second extremal photon radius is larger than r_- , and thus outside the naked singularity.

The radial transformation that casts the metric in the form (3.27) that makes the projective symmetry manifest can be integrated to give:

$$u = \frac{1}{r_-} \frac{1+a^2}{1-a^2} \left(1 - F_-^{\frac{1-a^2}{1+a^2}} \right), \quad (4.26)$$

with $F_{\pm} = 1 - \frac{r_{\pm}}{r}$. This equation can then be inverted, to give r in terms of u . We have already shown that

$$k(u) = \frac{1}{R_{\text{opt}}^2} = \frac{1}{r^2} F_+ F_-^{\frac{1-3a^2}{1+a^2}} - \lambda \quad (4.27)$$

has a cosmological constant contribution that is independent of the radial coordinate. The $a = 0$ case is special, with

$$u = -\frac{1}{r_-} \log\left(1 - \frac{r_-}{r}\right). \quad (4.28)$$

5 Black Holes in Horndeski Gravity

In this section we examine the static black hole solutions in a simple example of a Horndeski theory of gravity coupled to a scalar field, and we show that in certain cases there can be two photon spheres outside the black hole horizon. Specifically, we consider the theory

described by the Lagrangian

$$\mathcal{L} = \sqrt{-g} \left[R - 2\Lambda - \frac{1}{2}(\alpha g^{\mu\nu} - \gamma G^{\mu\nu}) \partial_\mu \chi \partial_\nu \chi \right], \quad (5.1)$$

where $G_{\mu\nu} = R_{\mu\nu} - \frac{1}{2}Rg_{\mu\nu}$ is the Einstein tensor. In four dimensions, the black hole is given by [42, 43]

$$\begin{aligned} ds^2 &= -h dt^2 + \frac{dr^2}{f} + r^2 d\Omega_2^2, & \chi'^2 &= \frac{3\beta g^2 r^2}{(1 + 3g^2 r^2) f}, \\ h &= C - \frac{\mu}{r} + g^2 r^2 + \frac{D \arctan(\sqrt{3}gr)}{\sqrt{3}gr}, & f &= \frac{(4 + \beta\gamma)^2 (1 + 3g^2 r^2)^2}{[4 + 3(4 + \beta\gamma)g^2 r^2]^2} h, \end{aligned} \quad (5.2)$$

where

$$C = \frac{4 - \beta\gamma}{4 + \beta\gamma}, \quad D = \frac{\beta^2 \gamma^2}{(4 + \beta\gamma)^2}, \quad (5.3)$$

and the constants g and β are related to α , γ and Λ by

$$\alpha = 3g^2 \gamma, \quad \Lambda = -3g^2 (1 + \frac{1}{2}\beta\gamma). \quad (5.4)$$

Defining

$$G(x) \equiv \frac{\arctan x}{x}, \quad (5.5)$$

and letting $x = \sqrt{3}gr$, the horizon is located at $r = r_0$ (and hence $x = x_0$) where

$$0 = -\frac{\mu}{r_0} + C + (g^2 r_0^2 + DG(x_0)). \quad (5.6)$$

Now $3x^2 + G(x) - 1 \geq 0$, and $D \leq 1$, and so it follows that

$$g^2 r^2 + DG(\sqrt{3}gr) \geq (g^2 r^2 + DG(\sqrt{3}gr)) \Big|_{g=0}, \quad (5.7)$$

and so the radius r_0 of the horizon for general g is smaller than the radius when $g = 0$, implying

$$r_0 \leq \frac{\mu}{C + D} = \frac{16\mu}{(4 + \beta\gamma)^2}. \quad (5.8)$$

The photon sphere is determined by finding the root or roots of $(R^{-2})' = 0$ that lie outside the horizon, where $R^2 = r^2/h$ is the radius-squared in the optical metric. Note that unlike all the previous black hole examples, here $(R^{-2})'$ is dependent on the ‘‘gauge coupling’’ g that determines the effective AdS cosmological constant, since it enters in the function $G(\sqrt{3}gr)$. Setting $(R^{-2})' = 0$ we obtain an expression that can be written as

$$1 - \frac{3\mu}{2(C + D)r} = \frac{D}{2(C + D)} \left[\frac{3 + 2x^2}{1 + x^2} - \frac{3 \arctan x}{x} \right]. \quad (5.9)$$

The function in square brackets on the right-hand side can be shown to be non-negative, and hence we have the result that the radius r_s of the photon sphere obeys the inequality

$$r_s \geq \frac{3\mu}{2(C + D)} = \frac{24\mu}{(4 + \beta\gamma)^2}. \quad (5.10)$$

In view of (5.8), we see that the photon sphere must lie outside the horizon, with

$$r_s \geq \frac{3}{2}r_0. \quad (5.11)$$

We can write (5.9) as

$$\frac{32}{\beta^2\gamma^2} - \frac{3\sqrt{3}g\mu(4+\beta\gamma)^2}{\beta^2\gamma^2x} = \frac{3+2x^2}{1+x^2} - \frac{3\arctan x}{x}, \quad (5.12)$$

and since the right-hand side ranges monotonically from 0 to 2 as x ranges from 0 to infinity, it follows that there will generically be two solutions or none if $32/(\beta^2\gamma^2) < 2$ (depending on the value of μ), and one solution or none if $32/(\beta^2\gamma^2) > 2$ (again, depending on the value of μ).

6 Quintessence Black Holes

According to [44], quintessence should satisfy

$$T_{\hat{\phi}\hat{\phi}} = T_{\hat{\theta}\hat{\theta}} = -\frac{1}{2}(3w+1)T_{\hat{r}\hat{r}} = \frac{1}{2}(3w+1)T_{\hat{t}\hat{t}}, \quad (6.1)$$

where w is taken to be a constant. The dominant energy condition [45] requires $T_{\hat{t}\hat{t}} \geq 0$ and

$$|3w+1| \leq 2. \quad (6.2)$$

It follows from (2.29) that γ in the metric (2.27) is constant, and hence, by rescaling t appropriately,

$$-g_{tt} = \frac{1}{g_{RR}} = \frac{1}{1 - \frac{2M(R)}{R}}, \quad (6.3)$$

where R is the area distance. $M(R)$ is called the Misner-Sharp mass. For further discussion of (6.3) see [46]. One then has

$$\frac{2M(R)}{R} = \frac{2M_0}{R} + \epsilon \left(\frac{L_w}{R}\right)^{3w+1}. \quad (6.4)$$

The values $(w, \epsilon) = (\frac{1}{3}, -1)$ corresponds to the Reissner-Nordström metric. If $(w, \epsilon) = (-1, \pm 1)$, one has a cosmological constant. Kiselev [44] favours, on symmetry grounds, $(w, \epsilon) = (-\frac{2}{3}, 1)$ for quintessence which, as a consequence, satisfies the dominant energy condition. Under this assumption, the metric is given by

$$ds^2 = -\left(1 - \frac{2M}{R} - \frac{R}{L}\right)dt^2 + \frac{dr^2}{1 - \frac{2M}{R} - \frac{R}{L}} + R^2(d\theta^2 + \sin^2\theta d\phi^2). \quad (6.5)$$

If $M = 0$ we obtain a metric reminiscent of de Sitter space, with a cosmological event horizon at $R = L$ and a naked singularity at $R = 0$. The optical radius R_{opt} is given by

$$\frac{1}{R_{\text{opt}}^2} = \frac{1}{R^2} - \frac{1}{LR}, \quad (6.6)$$

and so

$$\frac{d}{dR}\left(\frac{1}{R_{\text{opt}}^2}\right) = -\frac{1}{R^3}\left(2 - \frac{R}{L}\right), \quad (6.7)$$

which is negative throughout the static region.

One may take L negative; $L = -a$ say. This corresponds to quintessence with a negative energy density. The metric no longer has a cosmological horizon, but it does not have AdS asymptotics, but, rather, something softer. Defining

$$\rho + a = a\sqrt{1 + \frac{R}{a}}, \quad (6.8)$$

so that if

$$R = r + \frac{r^2}{4a}, \quad (6.9)$$

the metric becomes

$$ds^2 = -dt^2 + dr^2 + r^2\left(1 + \frac{r}{4a}\right)^2(d\theta^2 + \sin^2\theta d\phi^2). \quad (6.10)$$

In the positive r direction, the area of a sphere of constant radius increases faster than it would in flat space, but more slowly than in AdS₄. In the negative r direction we get the solution for ordinary quintessence with a cosmological horizon. The solution has a singularity at $r = 0$. This is clear, since R^2 as a function of r has odd powers of r , starting with an r^3 term.

We turn now to the quintessence black hole (6.5) with $M > 0$. If $M < L/8$ then there are two Killing horizons, at

$$R = R_{H_{\mp}} = \frac{1}{2}L\left(1 \mp \sqrt{1 - \frac{8M}{L}}\right) = \frac{1}{2}L\left(1 \mp \sqrt{1 - 8x}\right), \quad (6.11)$$

where $x = M/L$. These horizons coalesce at $R = \frac{L}{2}$ when $M = L/8$, or $x = 1/8$.

Provided $M < L/6$, i.e. $x < 1/6$, which of course is always greater than the critical value $x = 1/8$, the derivative

$$\frac{d}{dR}\left(\frac{1}{R_{\text{opt}}^2}\right) = \frac{1}{LR^4}(R^2 - 2RL + 6ML) \quad (6.12)$$

vanishes at

$$R = \bar{R}_{\mp} = L\left(1 \mp \sqrt{1 - \frac{6M}{L}}\right) = L\left(1 \mp \sqrt{1 - 6x}\right). \quad (6.13)$$

Now $-g_{tt}$ vanishes at the horizons $R = R_{H_{\mp}}$. Thus we expect an odd number of critical points in the static interval $R_{H_-} < R < R_{H_+}$. Since we have two solutions, we therefore expect that one will lie inside the static region and one outside. In order to see which we calculate

$$\bar{R}_- - R_{H_-} = \frac{L}{2}(1 - f(x)) \quad (6.14)$$

$$\bar{R}_+ - R_{H_+} = \frac{L}{2}(1 + f(x)), \quad (6.15)$$

where the function

$$f(x) := 2\sqrt{1-6x} - \sqrt{1-8x} \quad (6.16)$$

is defined on the interval $0 \leq x \leq \frac{1}{8}$. Clearly

$$f(0) = f\left(\frac{1}{8}\right) = 1, \quad f'(x) = -\frac{6}{\sqrt{1-6x}} + \frac{4}{\sqrt{1-8x}}. \quad (6.17)$$

Any critical point of $f(x)$ must satisfy

$$9(1-8x) = 4(1-6x) \quad (6.18)$$

There is a unique such x , namely

$$x = \frac{5}{48}, \quad f\left(\frac{5}{48}\right) = \sqrt{\frac{2}{3}}, \quad (6.19)$$

and hence

$$\sqrt{\frac{2}{3}} \leq f(x) \leq 1, \quad (6.20)$$

and so

$$1 \pm f(x) \geq 0. \quad (6.21)$$

Thus

$$R_{H_-} \leq \bar{R}_- \leq R_{H_+} \leq \bar{R}_+. \quad (6.22)$$

Hence we obtain a single photon sphere, with the larger critical point lying beyond the cosmological horizon. There is no anti-photon sphere.

7 Higher Dimensions

7.1 Five dimensions

The metric of the static three-charge black hole solution of the maximally supersymmetric gauged supergravity [33, 47] takes the form

$$ds^2 = -(H_1 H_2 H_3)^{-2/3} f dt^2 + (H_1 H_2 H_3)^{1/3} \left(f^{-1} dr^2 + r^2 d\Omega_3^2 \right), \quad (7.1)$$

where

$$f = 1 - \frac{2m}{r^2} + g^2 r^2 H_1 H_2 H_3 \quad H_i = 1 + \frac{q_i}{r^2}, \quad i = 1, 2, 3. \quad (7.2)$$

The mass and three U(1) charges are given by:

$$M_{ADM} = m + \frac{1}{3} \sum_{i=1}^3 q_i, \quad Q_i^2 = q_i(q_i + 2m), \quad i = 1, 2, 3. \quad (7.3)$$

Using (7.1), we see that the three-charge black hole in AdS₅ has an optical radius $R_{\text{opt}}(r)$ given by

$$\frac{1}{R_{\text{opt}}^2} = \frac{1}{r^2 H_1 H_2 H_3} \left(1 - \frac{2m}{r^2} + g^2 r^2 H_1 H_2 H_3 \right) = \frac{1}{r^2 H_1 H_2 H_3} \left(1 - \frac{2m}{r^2} \right) + g^2. \quad (7.4)$$

The situation is very similar to that in four spacetime dimensions. The extremum is determined by the equation

$$\frac{r^2 - 4m}{r^2 - 2m} = \sum_{i=1}^3 \frac{q_i}{r^2 + q_i}, \quad (7.5)$$

which has a unique positive solution with $r^2 = \bar{r}^2 > 4m$.

A generalization Hod's theorem (2.45) to higher dimensions, given in [22], can be shown to be satisfied for these solutions. Namely, one can write

$$\bar{R}^2 = \prod_{i=1}^3 (\bar{r}^2 + q_i)^{\frac{1}{3}} \leq \frac{1}{3} \sum_{i=1}^3 (\bar{r}^2 + q_i) \leq \frac{1}{3} \sum_{i=1}^3 (4m + q_i) = 4M_{ADM} + \bar{r}^2 - 4m - \sum_{i=1}^3 q_i \leq 4M_{ADM}. \quad (7.6)$$

The first inequality above is due to the inequality of geometric and arithmetic means, and the second inequality follows from:

$$\bar{r}^2 - 4m - \sum_{i=1}^3 q_i = - \sum_{i=1}^3 \frac{q_i (q_i + 2m)}{\bar{r}^2 + q_i} \leq 0, \quad (7.7)$$

where the first equality above is due to (7.5).

7.2 Seven dimensions

The static two-charged black hole in an AdS₇ background given in [33] has the metric

$$- (H_1 H_2)^{-\frac{4}{5}} f dt^2 + (H_1 H_2)^{\frac{1}{5}} \left(\frac{dr^2}{f} + r^2 d\Omega_5^2 \right), \quad (7.8)$$

with

$$f = 1 - \frac{2m}{r^4} + g^2 r^2 H_1 H_2, \quad H_i = 1 + \frac{q_i}{r^4}, \quad i = 1, 2. \quad (7.9)$$

The mass and two U(1) charges are given by:

$$M_{ADM} = m + \frac{2}{5} \sum_{i=1}^2 q_i, \quad Q_i^2 = q_i (q_i + 2m), \quad i = 1, 2. \quad (7.10)$$

The optical radius $R_{\text{opt}}(r)$ is given by

$$\frac{1}{R_{\text{opt}}^2} = \frac{1}{r^2 H_1 H_2} \left(1 - \frac{2m}{r^4} + g^2 r^2 H_1 H_2 \right) = \frac{1}{r^2 H_1 H_2} \left(1 - \frac{2m}{r^4} \right) + g^2. \quad (7.11)$$

and the argument goes through as in the previous example. The extremum is determined by the equation

$$\frac{r^4 - 6m}{r^4 - 2m} = \sum_{i=1}^2 \frac{2q_i}{r^4 + q_i}, \quad (7.12)$$

which has a unique positive solution with $r^4 = \bar{r}^4 > 6m$.

It can be shown that these solutions satisfy an analog of Hod's theorem (2.45), generalised to seven dimensions [22]. Namely, we write

$$\bar{R}^4 = [\bar{r}^4 \prod_{i=1}^2 (\bar{r}^4 + q_i)^2]^{\frac{1}{5}} \leq \frac{1}{5} [\bar{r}^4 + 2(\bar{r}^4 + q_1) + 2(\bar{r}^4 + q_2)] \leq 6M_{ADM} + \bar{r}^4 - 6m - 2 \sum_{i=1}^2 q_i \leq 6M_{ADM}. \quad (7.13)$$

The first inequality above is due to the inequality of geometric and arithmetic means. The second inequality is due to:

$$\bar{r}^4 - 6m - 2 \sum_{i=1}^2 q_i = -2 \sum_{i=1}^2 \frac{q_i(q_i + 2m)}{\bar{r}^4 + q_i} \leq 0, \quad (7.14)$$

where the first equality above is due to (7.12).

8 Conclusions

In this paper we have examined the optical metrics of static spherically symmetric solutions of various theories of current interest. In particular we have been interested in whether they admit photon spheres and if so how many. In the case of all the solutions we have looked at whose energy momentum tensor satisfies the dominant and strong energy conditions and which are non-singular outside a regular event horizon we have found a unique photon sphere and as a consequence no anti-photon spheres. For some ultra-extremal solutions we have found, consistent with other authors one may have both a photon sphere and an anti-photon sphere. We have also found in the case of a particular theory of Horndeski type that one may have both a photon sphere and an anti-photon sphere outside a regular Killing horizon of the spacetime metric. We are thus lead to the conjecture that a violation of the either the dominant or the strong energy condition is a necessary condition for the existence of an anti-photon sphere outside a regular black hole horizon.

We have investigated a conjecture of Hod [8], concerning a lower bound on the optical radius of the photon sphere (see eqn (2.50)), and found counterexamples in the case of static black holes in STU supergravity where fewer than three electric charges are turned on.

We have also found that that the rather mysterious projective symmetry of the optical metric first observed in the case of the Schwarzschild de Sitter metric continues to hold for the static spherically symmetric solutions of the STU supergravity theories. At present we have no conceptual understanding of why this symmetry is present, nor why it seems related to the fact that the null geodesics in this case may be described by Weierstrass elliptic functions.

9 Acknowledgements

We are grateful to Emanuel Gallo, Sharhar Hod and Claude Warnick for some helpful remarks. The work of M.C. is supported in part by the DOE (HEP) Award de-sc0013528, the Fay R. and Eugene L. Langberg Endowed Chair (M.C.) and the Slovenian Research Agency (ARRS). The work of C.N.P. is supported in part by DOE grant DE-FG02-13ER42020. G.W.G. is grateful for the award of a LE STUDIUM Chair held at the LMPT of the University of Tours under the auspices of which some of the work described in this paper was carried out. M.C. and C.N.P. are grateful the University of Tours and Beijing Normal University for hospitality during the course of the work.

A k-Essence and Irrotational Relativistic Fluids

The equation of motion for the theory with Lagrangian $L = L(X)$, where $X = -g^{\mu\nu}\partial_\mu\psi\partial_\nu\psi$, is given by

$$\nabla_\mu\left(\frac{\partial L}{\partial X}\nabla^\mu\psi\right) = 0. \quad (\text{A.1})$$

We may define a current

$$J^\mu = \frac{\partial L}{\partial X}\nabla^\mu\psi, \quad (\text{A.2})$$

which is conserved by virtue of the shift symmetry $\psi \rightarrow \psi + \text{constant}$. If $L_X = \frac{\partial L}{\partial X}$, then the energy-momentum tensor is

$$T_{\mu\nu} = 2L_X\partial_\mu\psi\partial_\nu\psi + g_{\mu\nu}L \quad (\text{A.3})$$

If $X > 0$ we may define a unit timelike vector by

$$u_\mu = \frac{\partial_\mu\psi}{\sqrt{X}}, \quad (\text{A.4})$$

and find that the energy-momentum tensor takes the form of an irrotational perfect fluid with Eulerian 4-velocity u_μ :

$$T_{\mu\nu} = \rho u_\mu u_\nu + P(g_{\mu\nu} + u_\mu u_\nu), \quad (\text{A.5})$$

where

$$\rho + P = 2XL_X, \quad P = L, \quad \rho = 2XL_X - L. \quad (\text{A.6})$$

Here $g_{\mu\nu} + u_\mu u_\nu = h_{\mu\nu}$ is a projection tensor which projects an arbitrary vector to one orthogonal to the world lines of the fluid. A simple calculation yields

$$\frac{\partial\rho}{\partial P} = \frac{L_X - 2XL_{XX}}{L_X}, \quad (\text{A.7})$$

whence, as will be verified later, the sound speed v_s is given by

$$v_s^2 = \frac{L_X}{L_X - 2XL_{XX}}. \quad (\text{A.8})$$

Examples of k-essence include

- Polytropic fluid with $P = w\rho$

$$L = X^{\frac{1+w}{2w}} = X^p, \quad w = \text{constant} = \frac{1}{2p-1}, \quad (\text{A.9})$$

where p may be fractional. The left-hand side of the equation of motion

$$\nabla^\mu (X \nabla_\mu \psi) = 0 \quad (\text{A.10})$$

is what one might call p -D'Alembertian, the analogue in Lorentzian geometry of the p -Laplacian of Riemannian geometry. The case $p = 2$ in $d = 4$ is conformally invariant.

- Born Infeld:

$$L = -\sqrt{1 - \bar{X}} + 1, \quad P = \frac{\rho}{\rho + 1}. \quad (\text{A.11})$$

- The Chaplygin gas:

$$L = -\sqrt{1 - \bar{X}}, \quad P = -\frac{1}{\rho}. \quad (\text{A.12})$$

Of course the fluid description only works if $X > 0$ and so, in particular, it cannot be applied to static solutions, which have $X < 0$.

A.1 Thermodynamics

Since $u^\mu_{;\mu} = \dot{V}/V$, where V is the infinitesimal volume of an element of the fluid dragged along the flow lines, the first law of thermodynamics reads

$$(\rho + P)dV + Vd\rho = 0. \quad (\text{A.13})$$

Now in general, if a fluid is locally homogeneous and passes through thermodynamic equilibria, we have

$$Ts = \rho + P, \quad Tds = d\rho, \quad \frac{d\rho}{\rho + P} = \frac{ds}{s}. \quad (\text{A.14})$$

Therefore, by (A.13), we have

$$sV = \text{constant} \quad (\text{A.15})$$

and the flow is isentropic. From (A.14) the dependence of all (ρ, P, s, T) on any one of them is determined once an equation of state is specified, and hence by (A.13) on the volume expansion. Thus for a polytrope,

$$\rho = A \left(\frac{T}{1+w} \right)^{\frac{1+w}{w}}, \quad s = (1+w)A \left(\frac{T}{1+w} \right)^{\frac{1}{w}}, \quad (\text{A.16})$$

where A is a constant with dimensions $L^{-3} M^{-\frac{1}{w}}$. If $w = \frac{1}{3}$, A has dimensions $L^{-3} M^{-3} = \hbar^{-3}$. If $w \neq \frac{1}{3}$ one needs a further dimensionful constant to relate the energy density to the entropy density or to the temperature.

A.2 Entropy current as Noether current

The conserved current arising from the shift symmetry $\psi \rightarrow \psi + \text{constant}$ gives rise to a conserved current,

$$J^\mu = \frac{\partial L}{\partial(\partial_\mu \psi)} = -2X^{\frac{1}{2}} L_X u^\mu. \quad (\text{A.17})$$

From (A.7)

$$-2X^{\frac{1}{2}} L_X = -X^{-\frac{1}{2}} 2X L_X = -(\rho + P) X^{-\frac{1}{2}}, \quad (\text{A.18})$$

and from (A.14) we have

$$\frac{ds}{s} = \left(\frac{d\rho + dP}{\rho + P} - \frac{dP}{\rho + P} \right) \quad (\text{A.19})$$

$$= d \ln(\rho + P) - \frac{dL}{2X L_X} \quad (\text{A.20})$$

$$= d \ln(\rho + P) - \frac{dX}{2X}, \quad (\text{A.21})$$

whence

$$s = \text{constant} \times (\rho + P) X^{-\frac{1}{2}}. \quad (\text{A.22})$$

Thus

$$J^\mu = \text{constant} \times s u^\mu. \quad (\text{A.23})$$

For example, for radiation we have $w = \frac{1}{3}$, and hence

$$L = X^2 = (g^{\mu\nu} \partial_\mu \psi \partial_\nu \psi)^2. \quad (\text{A.24})$$

The equation of motion is

$$\nabla_\mu ((\nabla \psi)^2 \nabla^\mu \psi) = 0, \quad (\text{A.25})$$

or, as long as $\nabla^\mu \psi$ is timelike,

$$(g^{\mu\nu} - 2u^\mu u^\nu) \nabla_\mu \nabla_\nu \psi = 0. \quad (\text{A.26})$$

One recognizes

$$(a^{-1})^{\mu\nu} = g^{\mu\nu} - 2u^\mu u^\nu \quad (\text{A.27})$$

as the acoustic co-metric, i.e. the inverse of the acoustic metric

$$a_{\mu\nu} = g_{\mu\nu} + \frac{2}{3} u_\mu u_\nu \quad (\text{A.28})$$

for a fluid with $P = \frac{1}{3}\rho$.

If one repeats the calculation above for $L = X^p$, one finds

$$(a^{-1})^{\mu\nu} = g^{\mu\nu} - (2p-1)u^\mu u^\nu \quad (\text{A.29})$$

$$a_{\mu\nu} = g_{\mu\nu} + 1 - wu_\mu u_\nu, \quad (\text{A.30})$$

which corresponds to a fluid with sound speed $v_s = \sqrt{\frac{\partial P}{\partial \rho}} = \sqrt{w}$. For both the Born-Infeld and the Chaplygin gases, one finds the sound speed v_s to be given by

$$v_s = \sqrt{1-X} \quad (\text{A.31})$$

and

$$(a^{-1})^{\mu\nu} = g^{\mu\nu} - \frac{X}{1-X} u^\mu u^\nu \quad (\text{A.32})$$

$$a_{\mu\nu} = g_{\mu\nu} + X u_\mu u_\nu. \quad (\text{A.33})$$

In general one finds that the equation of motion for ψ takes the form

$$(a^{-1})^{\mu\nu} \nabla_\mu \nabla_\nu \psi = 0, \quad (\text{A.34})$$

where the acoustic co-metric $a^{-1\mu\nu}$ is given by

$$(a^{-1})^{\mu\nu} = g^{\mu\nu} - 2 \frac{L_{XX}}{L_X} u^\mu u^\nu. \quad (\text{A.35})$$

Equation (A.35) is consistent with (A.8):

$$\nabla_\mu ((\nabla\psi)^2 \nabla^\mu \psi) = 0, \quad (\text{A.36})$$

or, as long as $\nabla^\mu \psi$ is timelike,

$$(g^{\mu\nu} - 2u^\mu u^\nu) \nabla_\mu \nabla_\nu \psi = 0. \quad (\text{A.37})$$

A.3 Black hole accretion and emission

In order to describe a steady (i.e. time independent) spherically symmetric flow in a background whose metric is

$$ds^2 = -\Delta(R)dt^2 + \frac{dR^2}{F(r)} + R^2(d\theta^2 + \sin^2\theta d\phi^2) \quad (\text{A.38})$$

$$= \Delta \left\{ -dt^2 + dr_\star^2 + \frac{r^2}{\Delta} (d\theta^2 + \sin^2\theta d\phi^2) \right\} \quad (\text{A.39})$$

where the metric in the braces is the optical metric and r_\star is the radial optical distance, often called the the Regge-Wheeler tortoise coordinate:

$$dr_\star = \frac{dR}{\sqrt{F\Delta}}. \quad (\text{A.40})$$

We make the ansatz

$$\psi = t - \chi(R), \quad (\text{A.41})$$

and find that the fluid 3-velocity v with respect to a local orthonormal frame at rest with respect to the hole is given by

$$v = \frac{d\chi}{dr_*}. \quad (\text{A.42})$$

If $v > 0$, the flow is an outward-directed wind. If $v < 0$, we have an inward-directed accretion flow. Moreover

$$X = \frac{1}{\Delta(1-v^2)}. \quad (\text{A.43})$$

For any steady radial conserved current we have

$$R^2 \sqrt{\frac{\Delta}{F}} J_R = \text{constant}. \quad (\text{A.44})$$

In our case, if $d = 4$, that means

$$vR^2 L_X(X) = \text{constant} = vR^2 L_X\left(\frac{1-v^2}{\Delta}\right). \quad (\text{A.45})$$

For a polytropic gas this gives

$$v(1-v^2)^{p-1} = a^2 \frac{\Delta^{p-1}}{R^2} \quad (\text{A.46})$$

where a is a constant. As a varies, we obtain a family of curves in the (v, r) plane, labelled by the constant a . In the asymptotically-flat case, we are looking either for an ingoing curve or an outgoing curve.

It is a simple matter to check that (A.46) with $p = 2$ reproduces equation (15) of [20]. In the Schwarzschild case

$$\Delta = F = 1 - \frac{2M}{R}, \quad (\text{A.47})$$

one finds that if R is plotted against v for different values of the constant a , one obtains Figure 1 of [20]. The left-hand side of (A.46) with $p = 2$ achieves its greatest (least) value of $\pm \frac{2}{\sqrt{27}}$ at $v = \frac{d\chi}{dr_*} = \pm \frac{1}{\sqrt{3}}$. In other words the fluid velocity coincides with the velocity of sound. The right-hand side of (A.46) achieves its greatest (least) value when the optical radius

$$R_{\text{opt}} = \frac{R}{\sqrt{\Delta}} \quad (\text{A.48})$$

is stationary: In other words, at radii for which there are circular null geodesics. In order that v be a single-valued function of r on the interval $r \in (2M, \infty)$, we must therefore choose

$$\text{constant} = \pm 2\sqrt{27}M^2, \quad (\text{A.49})$$

$$v(1-v^2) = \pm 2\sqrt{27}M^2 \frac{\Delta}{R^2}. \quad (\text{A.50})$$

The Bondi radius, at which the two flows, one inward (-) and one outward (+), make a transition from subsonic to supersonic, occurs at the photon sphere $R = 3M$.

If the constant is positive we have a wind, whilst if the constant is negative we have accretion. Asymptotically we have

$$\text{wind (+): } R \rightarrow \infty \quad v = 1 - \sqrt{27}\left(\frac{M}{R}\right)^2 + \dots, \quad (\text{A.51})$$

$$r \rightarrow 2M \quad v = \frac{\sqrt{27}(R - 2M)}{4M} + \dots, \quad (\text{A.52})$$

$$\text{accretion (-): } R \rightarrow \infty \quad v = -2\sqrt{27}\left(\frac{M}{R}\right)^2 + \dots, \quad (\text{A.53})$$

$$r \rightarrow 2M \quad v = -1 + \frac{\sqrt{27}(R - 2M)}{8M} + \dots. \quad (\text{A.54})$$

Near the acoustic horizon we have

$$\text{wind (+): } R \rightarrow 3M \quad v = \frac{1}{\sqrt{3}} + \sqrt{\frac{2}{27}}\left(\frac{R - 3M}{M}\right) + \dots, \quad (\text{A.55})$$

$$\text{accretion (-): } R \rightarrow 3M \quad v = -\frac{1}{\sqrt{3}} + \sqrt{\frac{2}{27}}\left(\frac{R - 3M}{M}\right) + \dots. \quad (\text{A.56})$$

The case for general p is similar. The left-hand side of (A.46) achieves its maximum for $v^2 = w$. The right-hand side reaches its maximum for

$$r_{\text{Bondi}} = \frac{1}{2}M\left(3 + \frac{1}{w}\right). \quad (\text{A.57})$$

The analogy that is often made is with a de Laval nozzle. The throat or waist of the hourglass-shaped nozzle is a sonic horizon, at which the speed of sound and the speed of the fluid coincide. In the present case, this throat is the waist at $R = 3M$ of the optical wormhole whose geometry interpolates between flat space as $r_{\star} \rightarrow +\infty$ to the event horizon at $r_{\star} \rightarrow -\infty$, where the geometry approaches that near the conformal infinity of hyperbolic three-space [18] and whose radius curvature is given by the surface gravity, or 2π times the Hawking temperature. As pointed out in [18], this behaviour is universal for all black holes, and now we see that equally universal is the fact the the sonic horizon coincides (for a radiation gas) with the photon sphere.

References

- [1] C. M. Claudel, K. S. Virbhadra and G. F. R. Ellis, *The geometry of photon surfaces*, J. Math. Phys. **42** (2001) 818, gr-qc/0005050.
- [2] J. Keir, *Slowly decaying waves on spherically symmetric spacetimes and an instability of ultracompact neutron stars*, arXiv:1404.7036 [gr-qc].

- [3] V. Cardoso, L. C. B. Crispino, C. F. B. Macedo, H. Okawa and P. Pani, *Light rings as observational evidence for event horizons: long-lived modes, ergoregions and nonlinear instabilities of ultracompact objects*, Phys. Rev. D **90** (2014) 4, 044069, arXiv:1406.5510 [gr-qc].
- [4] J. W. York, *Black hole thermodynamics and the Euclidean Einstein action*, Phys. Rev. D **33** (1986) 2092.
- [5] S. W. Hawking and D. N. Page, *Thermodynamics of black holes in anti-de Sitter space*, Commun. Math. Phys. **87** (1983) 577.
- [6] E. Witten, *Anti-de Sitter space and holography*, Adv. Theor. Math. Phys. **2** (1998) 253, hep-th/9802150.
- [7] M. M. Akbar and G. W. Gibbons, *Ricci-flat metrics with $U(1)$ action and the Dirichlet boundary-value problem in Riemannian quantum gravity and isoperimetric inequalities*, Class. Quant. Grav. **20** (2003) 1787, arXiv:hep-th/0301026.
- [8] S. Hod, *The fastest way to circle a black hole*, Phys. Rev. D **84** (2011) 104024, arXiv:1201.0068 [gr-qc].
- [9] S. Hod, *Upper bound on the radii of black-hole photon spheres*, Phys. Lett. B **727** (2013) 345.
- [10] W. L. Ames and K. S. Thorne, *The optical appearance of a star that is collapsing through its gravitational radius*, Astrophysical Journal **151** (1968) 659.
- [11] J. L. Synge, *The escape of photons from gravitationally intense stars*, Mon. Not. Roy. Astr. Soc. **131** (1966) 463.
- [12] W. H. Press, *Long wave trains of gravitational waves from a vibrating black hole*, Ap. J. **170** (1971) L015.
- [13] C. J. Goebel, *Comments on the “vibrations” of a black hole*, Ap. J. **172**, L95.
- [14] J. N. Islam, *The cosmological constant and classical tests of general relativity*, Phys. Lett. **97A** (1983) 239.
- [15] G. W. Gibbons, C. M. Warnick and M. C. Werner, *Light-bending in Schwarzschild-de Sitter: projective geometry of the optical metric*, Class. Quant. Grav. **25** (2008) 245009, arXiv:0808.3074 [gr-qc].
- [16] S. Casey, M. Dunajski, G. W. Gibbons and C. Warnick, *Optical metrics and projective equivalence*, Phys. Rev. D **83** (2011) 084047, arXiv:1101.4375 [gr-qc].

- [17] G. W. Gibbons, *No glory in cosmic string theory*, Phys. Lett. B **308** (1993) 237.
- [18] G. W. Gibbons and M. C. Werner, *Applications of the Gauss-Bonnet theorem to gravitational lensing*, Class. Quant. Grav. **25** (2008) 235009, arXiv:0807.0854 [gr-qc].
- [19] G. W. Gibbons and C. M. Warnick, *Universal properties of the near-horizon optical geometry*, Phys. Rev. D **79** (2009) 064031, arXiv:0809.1571 [gr-qc].
- [20] B. Carter, G. W. Gibbons, D. N. C. Lin and M. J. Perry, *Black hole emission process in the high energy limit*, Astron. Astrophys. **52** (1976) 427.
- [21] M. Cvetič and G. W. Gibbons, *Graphene and the Zermelo optical metric of the BTZ black hole*, Annals Phys. **327**, 2617 (2012), arXiv:1202.2938 [hep-th].
- [22] E. Gallo and J. R. Villanueva, *Photon spheres in Einstein and Einstein-Gauss-Bonnet theories and circular null geodesics in axially-symmetric spacetimes*, Phys. Rev. D **92**, no. 6, 064048 (2015), arXiv:1509.07379 [gr-qc].
- [23] M. Ewing and J. L. Wurzel, *Long range sound transmission*, Geol. Soc. Am. Mem. 27 (1948).
- [24] L. M. Brekhovskikh, *Acoustics of the Ocean*, Part 1, Joint Publications Research Series, 1975, chapters 4 & 5.
- [25] C. S. Morawetz, *Geometrical optics and the singing of whales*, Amer. Math. Monthly **85** (1978) 548.
- [26] M. Porrati and R. Rabadan, *Boundary rigidity and holography*, JHEP **0401** (2004) 034, hep-th/0312039.
- [27] C. B. Croke and P. Herreros, *Lens rigidity with trapped geodesics in two dimensions*, arXiv:1108.4938 [math.DG].
- [28] C. B. Croke, *Scattering rigidity with trapped geodesics*, arXiv:1103.5511 [math.DG].
- [29] E. T. Whittaker, *On Gauss's theorem and the concept of mass in general relativity*, Proc. Roy. Soc. Lond. A **149** (1935) 384.
- [30] S. Hod, *Hairy black holes and null circular geodesics*, Phys. Rev. D **84** (2011) 124030, arXiv:1112.3286 [gr-qc].
- [31] G. W. Gibbons and C. M. Warnick, *Dark energy and projective symmetry*, Phys. Lett. B **688** (2010) 337, arXiv:1003.3845 [gr-qc].

- [32] M. J. Duff and J. T. Liu, *Anti-de Sitter black holes in gauged $N = 8$ supergravity*, Nucl. Phys. B **554** (1999) 237, hep-th/9901149.
- [33] M. Cvetič and S. S. Gubser, *Phases of R-charged black holes, spinning branes and strongly coupled gauge theories*, JHEP **9904** (1999) 024, hep-th/9902195.
- [34] M. Cvetič, G. W. Gibbons and C. N. Pope, *Super-Geometrodynamics*, JHEP **1503** (2015) 029, arXiv:1411.1084 [hep-th].
- [35] M. Cvetič and D. Youm, *Dyonic BPS saturated black holes of heterotic string on a six torus*, Phys. Rev. D **53**, 584 (1996) doi:10.1103/PhysRevD.53.584 [hep-th/9507090].
- [36] M. Cvetič and D. Youm, *BPS saturated and nonextreme states in Abelian Kaluza-Klein theory and effective $N=4$ supersymmetric string vacua*,” In *Los Angeles 1995, Future perspectives in string theory* 131-147 [hep-th/9508058].
- [37] P. Pradhan and P. Majumdar, *Circular orbits in extremal Reissner-Nordström spacetimes*, Phys. Lett. A **375**, 474 (2011), arXiv:1001.0359 [gr-qc].
- [38] F. S. Khoo and Y. C. Ong, *Lux in obscuro: Photon Orbits of Extremal Black Holes Revisited*, arXiv:1605.05774 [gr-qc].
- [39] H. Lü, Y. Pang and C. N. Pope, *AdS Dyonic black hole and its thermodynamics*, JHEP **1311** (2013) 033, arXiv:1307.6243 [hep-th].
- [40] G. W. Gibbons and K. i. Maeda, *Black holes and membranes in higher dimensional theories with dilaton fields*, Nucl. Phys. B **298** (1988) 741.
- [41] C. J. Gao and S. N. Zhang, *Dilaton black holes in de Sitter or Anti-de Sitter universe*, Phys. Rev. D **70** (2004) 124019, hep-th/0411104.
- [42] A. Anabalón, A. Cisterna and J. Oliva, *Asymptotically locally AdS and flat black holes in Horndeski theory*, Phys. Rev. D **89** (2014) 084050, arXiv:1312.3597 [gr-qc].
- [43] X. H. Feng, H. S. Liu, H. Lü and C. N. Pope, *Black hole entropy and viscosity bound in Horndeski gravity*, JHEP **1511** (2015), arXiv:1509.07142 [hep-th].
- [44] V. V. Kiselev, *Quintessence and black holes*, Class. Quant. Grav. **20** (2003) 1187, gr-qc/0210040.
- [45] S. W. Hawking, *The conservation of matter in general relativity*, Commun. Math. Phys. **18** (1970) 301.

- [46] T. Jacobson, *When is $g_{tt}g_{rr} = -1$?*, Class. Quant. Grav. **24** (2007) 5717, arXiv:0707.3222 [gr-qc].
- [47] K. Behrndt, M. Cvetič and W.A. Sabra, *Nonextreme black holes of five-dimensional $N=2$ AdS supergravity*, Nucl. Phys. B **553**, 317 (1999) doi:10.1016/S0550-3213(99)00243-6 [hep-th/9810227].
- [48] J. R. Villanueva, J. Saavedra, M. Olivares and N. Cruz, *Photons motion in charged anti-de Sitter black holes*, Astrophys. Space Sci. **344** (2013) 437.
- [49] G. W. Gibbons and M. Vyska, *The application of Weierstrass elliptic functions to Schwarzschild null geodesics*, Class. Quant. Grav. **29** (2012) 065016, arXiv:1110.6508 [gr-qc].